Advanced Time Series Analysis: Computer Exercise 4

Autumn 21, 01622
Assignment 4
January 5, 2022

Magne Egede Rasmussen, s183963,
Nicolaj Hans Nielsen, s184335
Anton Ruby Larsen, s174356

Danmarks
Tekniske Universitet

Supervisor: Emma Margareta Viktoria Blomgren, PhD Student
DTU - Department of Applied Mathematics and Computer Science

Contents

1 Introduction

Critical parts of a modern grid are both step-up and step-down transformers. They are used respectively to minimise the loss of power in transport by emphasising the use of high voltage cables and to secure a safety environment for the end-users. The function of any transformer is to change the relationship between the incoming voltage and current and the outgoing voltage and current. In theoretical examples, transformers are often assumed to be ideal. This is not the case in the real world, where they often become the bottleneck in the energy supply of modern grids.

The temperature of the transformer winding is the limiting factor as overheating the transformer would make it fail. Depending on the transformer setup, the temperature depends on electrical factors and different local environmental factors such as ambient temperature or solar radiation. To make an optimal power schedule, it is crucial to have a model for the transformer temperature to ensure that the transformer will not fail and allow consumers to receive their requested power. We will explore which power and environmental variables that are essential to construct a model for the temperature of the transformer.

In this report, we will demonstrate, by the use of CTSM [1], how to set up an appropriate model for the temperature of a transformer winding. The best models are reported in the process, while the conclusion gives an overview of the general results.

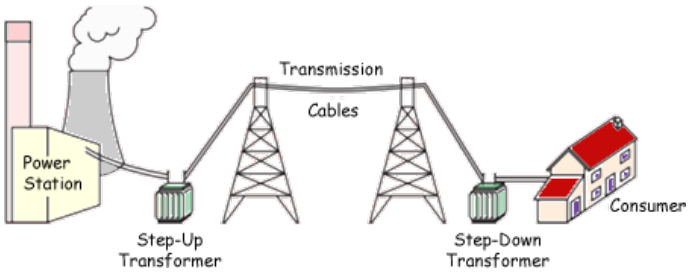

Figure 1.1 – Step up and step down transformers in a power grid.

1.1 Model Selection Criteria

Initially, we will force a small system variance to ensure that the models we construct can describe the dynamics of the system well. Using the level of variance, we will select the model with the lowest RSS and with the least amount of systematic variance in the residuals. To achieve a parsimonious model, we will use the BIC criterion in cases where we branch into models with increasing complexity. We will then increase the system variance with the final model and report the findings. In the progress of finding an optimal model, we also emphasize the importance of a realistic physical interpretation.

2 | Data Exploration

In this section, we take a close look at our given data sets. First, we highlight that we are given data from two different transformers. The two transformers are denoted respectively Transformer 1 and Transformer 2.

For the two transformers, the data is given in two different time periods. For Transformer 1 the interval is 01-11-2021 00:00 to 21-11-2021 19:30, while for Transformer 2 the time interval is truncated and lies in the span 10-11-2021 00:00 to 30-11-2021 11:30. For both transformers, the sampling rate is 30 minutes. In the table below, we briefly describe the given variables together with an example of a sample:

Name	Description	Unit	Example (index 20)
timedate	Date and time	YYYY-MM-DD hh:mm	2021-11-01 09:30
timestamp	timedate in seconds	s	1635756600
t	Time since start	s	34200
yT_ℓ	Temperature of the lid	C°	25.97
T_a	Ambient temperature	C°	10.89
$\mathrm{I1}_{sq}$	Squared current through line 1	I^2	14375.55
$\mathrm{I2}_{sq}$	Squared current through line 2	I^2	18341.26
$\mathrm{I3}_{sq}$	Squared current through line 3	I^2	16107.03
IN_{sq}	Squared current through the neutral line	I^2	0.108081
P_h	normalize($\mathrm{I1}_{sq} + \mathrm{I2}_{sq} + \mathrm{I3}_{sq}$)	I^2	0.044049
G_h	Normalized global radiation	W/m^2	0.390326
windN	Normalized wind speed if wind in north	m/s	0
windE	Normalized wind speed if wind in east	m/s	0
windS	Normalized wind speed if wind in south	m/s	0.526881
windW	Normalized wind speed if wind in west	m/s	0

Table 2.1 – Description of data available for modelling the transformer. Additionally, index 20 from Transformer 1 has been included to illustrate the structure of the data set.

2.1 Correlations

We start searching for correlations in data to find patterns to apply in our models. Our correlation matrices are shown on the next two pages. We have separated Transformer 1 and 2 and analysed them individually as we see some interesting differences between the two. In general, we highlight:

- The distribution of yT_ℓ are similar for the two transformers.
- The current variables are all very correlated for Transformer 1, which is not the the case for Transformer 2. The low correlation is primarily caused by $\mathrm{I3}_{sq}$.
- Wind speed and direction can not alone describe yT_ℓ for either Transformer 1 nor 2.

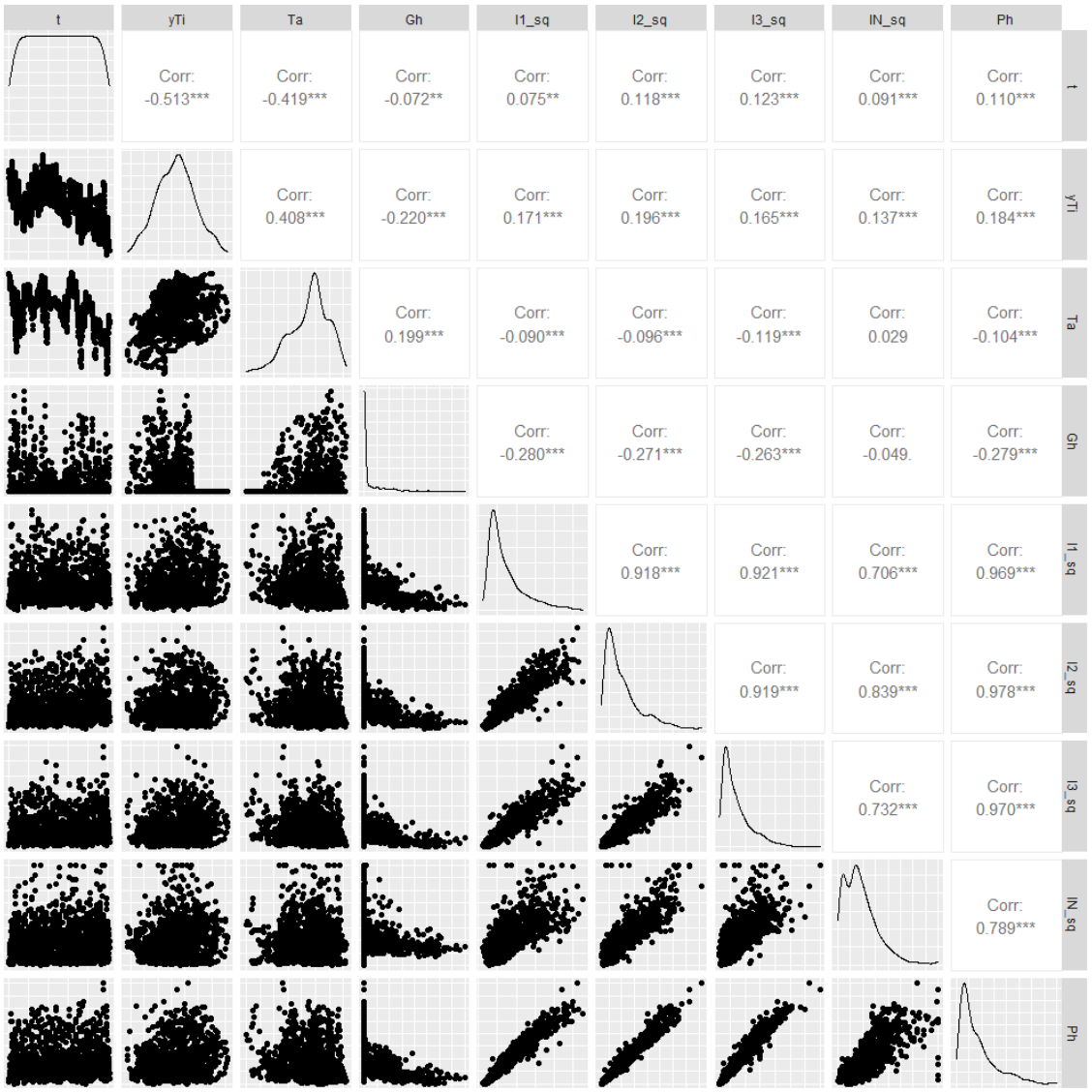

Figure 2.1 – Correlation Matrix: Transformer 1

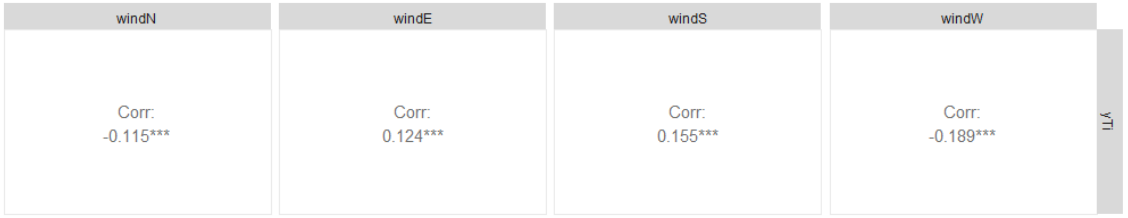

Figure 2.2 – Correlation with wind direction: Transformer 1

We highlight some specific results from Transformer 1:

- Ambient temperature is an important parameter determining lid temperature yT_ℓ.
- The lid temperature are generally higher when the sun does not shine. The result indicates that load-loss carry a lot of information about yT_ℓ and further that current impact peaks outside of working hours.

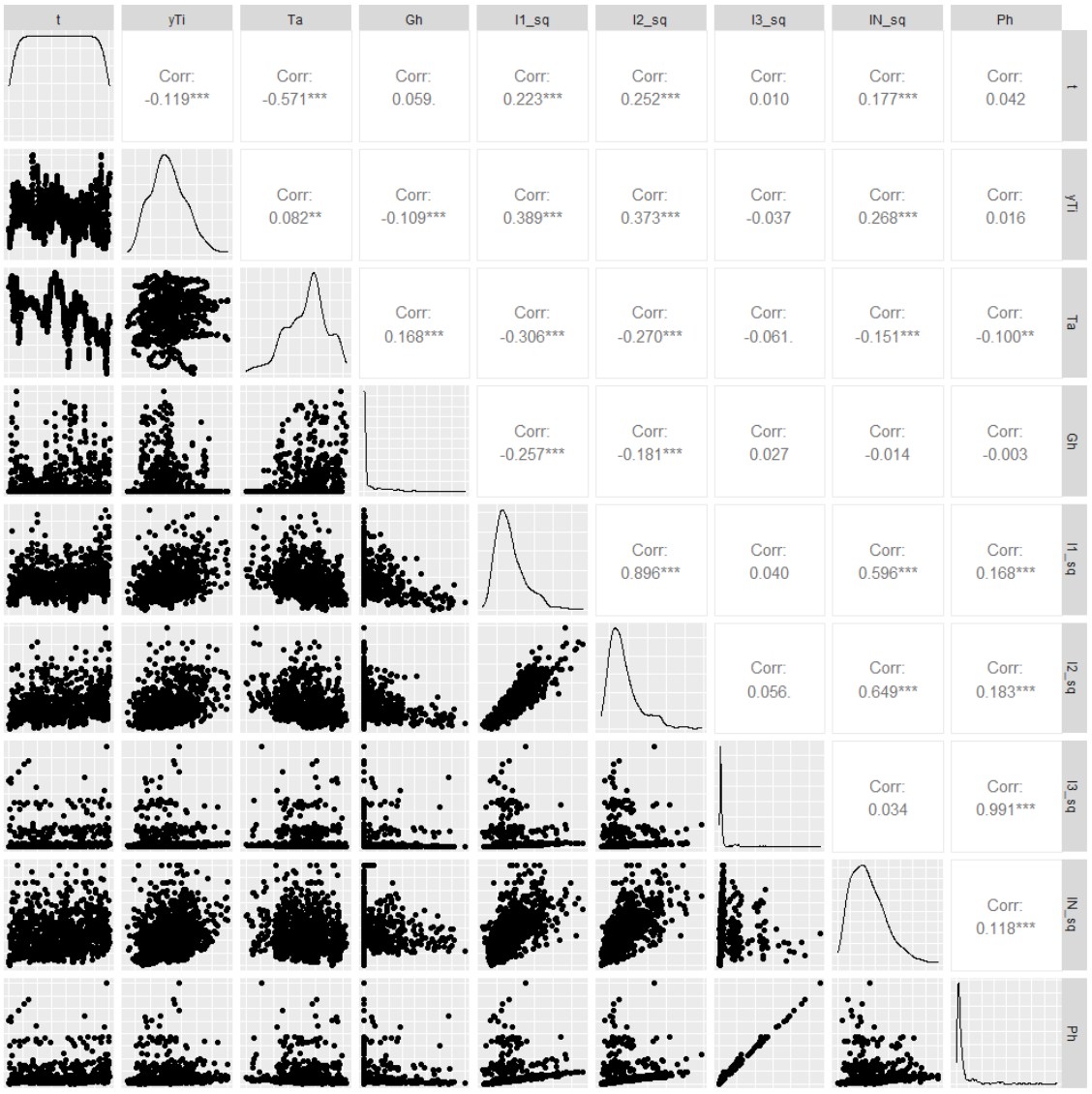

Figure 2.3 – Correlation Matrix: Transformer 2

Figure 2.4 – Correlation with wind direction: Transformer 2

Some specific results for Transformer 2:

- Ambient temperature does not seem to be as good of a predictor for the lid temperature yT_ℓ. It seems that the relationship should be studied further.
- P_h does not seem as an important parameter for Transformer 2, which potentially is due to the lack of correlation between $\mathrm{I3}_{sq}$ and yT_ℓ.

2.2 Solar Radiation & Wind

Solar radiation and wind are meteorological variables included in the data set. We take both into account as we suspect the transformer shed not to form a closed system. We study them individually in the following.

2.2.1 Introduction to Solar Radiation

Solar radiation is denoted by G_h. Based on section 2.1, we conclude that it is positively correlated with ambient temperature while negatively correlated with lid temperature. G_h has densities as in fig. 2.5, while the daily variations is shown in fig. 2.6.

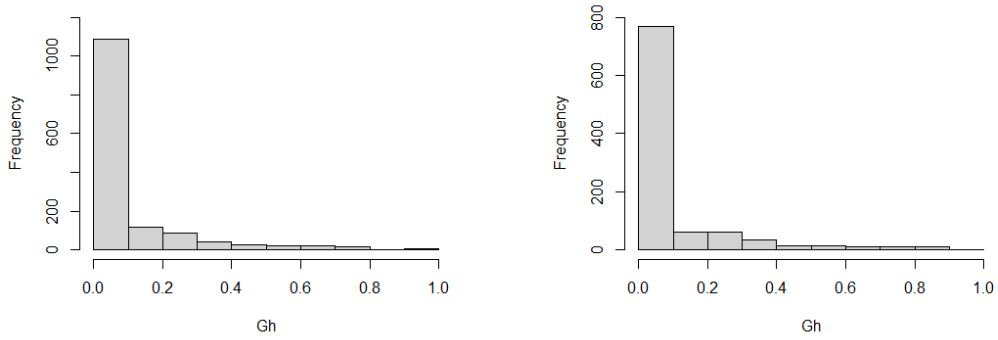

(a) Transformer 1 **(b)** Transformer 2

Figure 2.5 – Solar radiation distributions.

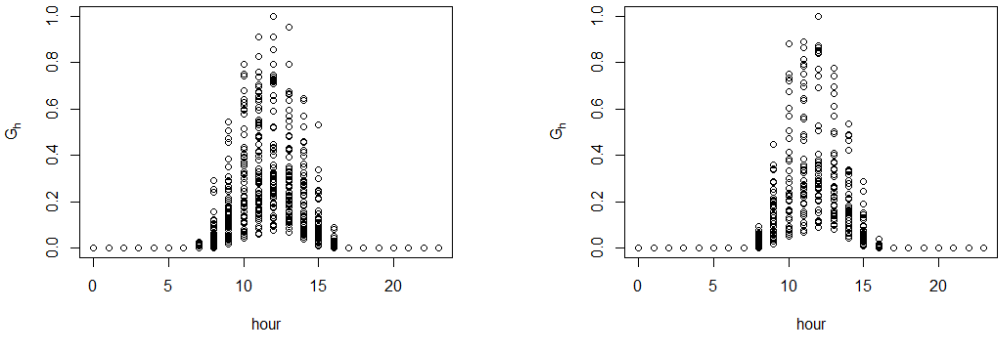

(a) Transformer 1 **(b)** Transformer 2

Figure 2.6 – Solar radiation daily variations.

2.2.2 Introduction to Wind Speed & Direction

For the specific data sets we have been given the parameters wind speed and an angular wind direction for each time step. The parameters are combined for the plots fig. 2.7 and fig. 2.8 illustrating that the average wind comes from south-west, while heavy winds arrive from north-west. From the Beaufort scale we see that the reported wind speed primarily lies between light breeze to moderate breeze with a maximum speed up to a moderate gale. We introduce four cardinal directions as the variables windN, windE, windS and windW. We do this to simplify the signal and be able to accommodate a general case, where only cardinal directions are given. Further, it aligns with the geometrical form of the shed.

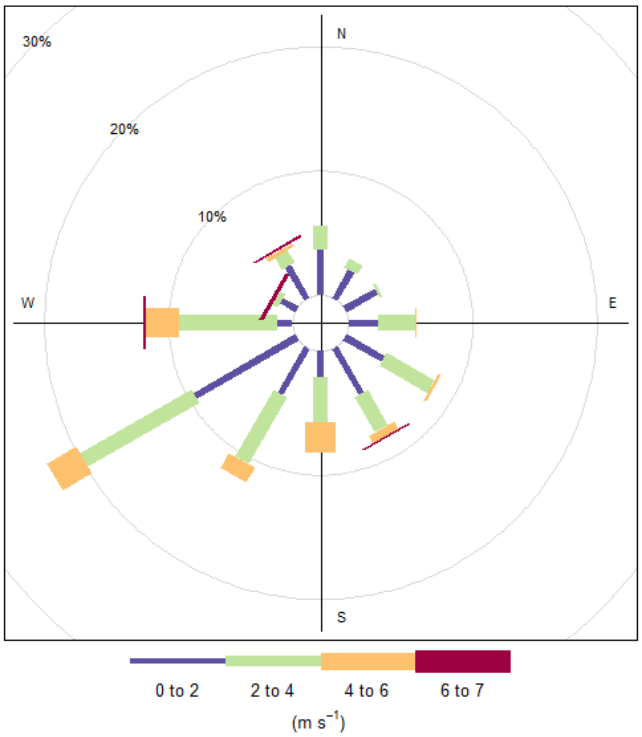

Figure 2.7 – WindRose Transformer 1

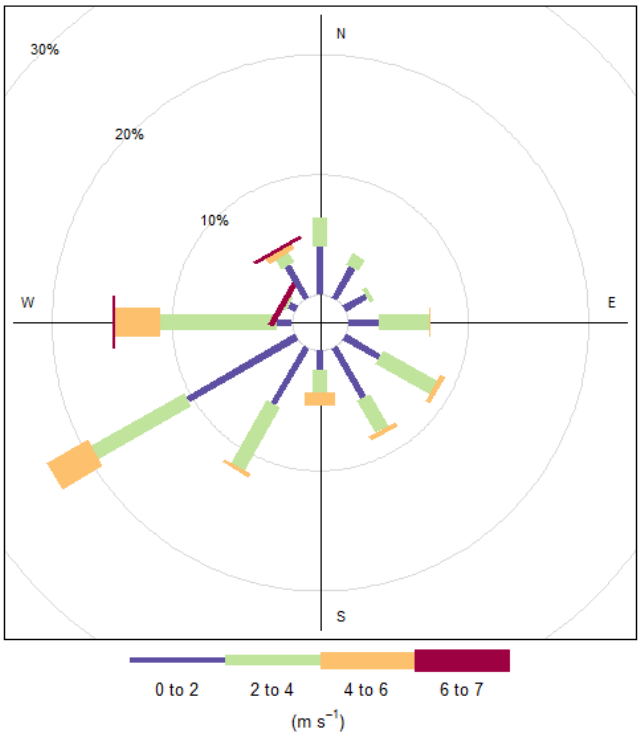

Figure 2.8 – WindRose Transformer 2

2.3 Introduction to Power Variables

The danish electrical grid is a 3-phase electrical grid. A 3-phase system typically employs 4 wires, one for each phase and a neutral return wire, as described in [2]. This is illustrated in figure 2.9. We will first dive into the three phases to understand these.

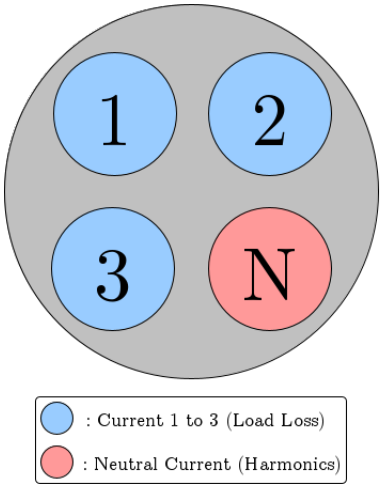

Figure 2.9 – A cross section of a typical power cable in a 3-phase system

2.3.1 Power Phases

Power is fed into the danish system by 3-phase generators with a frequency of 50 Hz, described in [3]. They work by spinning a magnet past three electromagnetic coils separated by 120 degrees, as illustrated in figure 2.10.

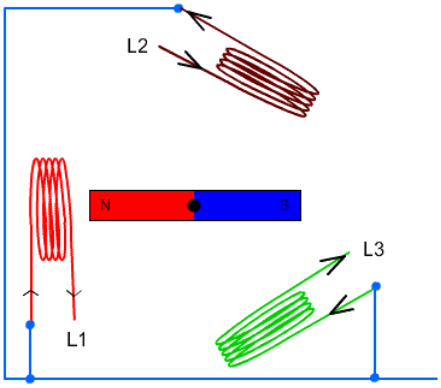

Figure 2.10 – Illustration of a 3-phase generator.

This generates three sine waves, each shifted 120 degrees. These are what we call the 3 phases in figure 2.9 and is illustrated in figure 2.11.

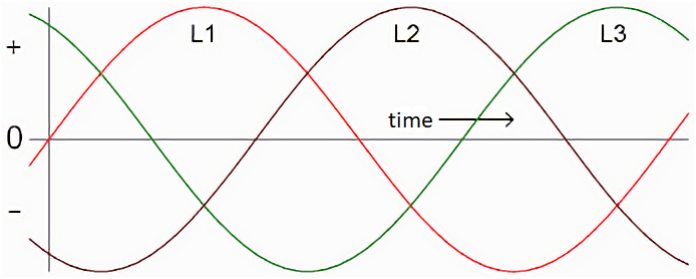

Figure 2.11 – Three power curves separated by 120 degrees.

2.3.2 Harmonics

We now dive into the role of the neutral return wire. In a linear system the neutral wire only carries current due to imbalances between the 3 phases. In our system today though we have a lot of nonlinear distortions for which a large portion is due to switch-mode power supplies, described in [2] under non-linear loads. These power supplies draws current in non-sinusoidal pulses giving a lot of different wave forms.

These wave forms can be split up into what is called harmonics. Harmonics are sinusoidal waves whose frequencies are an integer multiple of the fundamental frequency in the system, i.e. the frequency of the three phases.

Due to EV's, PV's and all the electrical equipment we use in our everyday life these switch-mode power supplies are becoming a larger and larger problem and hence we will also consider the heat contribution from the neutral line in our model selection.

2.3.3 Power Variables in Data

In our data set we are provided with variables for which we can extract the current in each phase and the harmonics described above. The variables are the current squared for each phase including the neutral return wire and are denoted $I1_{sq}$, $I2_{sq}$, $I3_{sq}$, IN_{sq}. In the following, we highlight difference in the phases for Transformer 1 and 2.

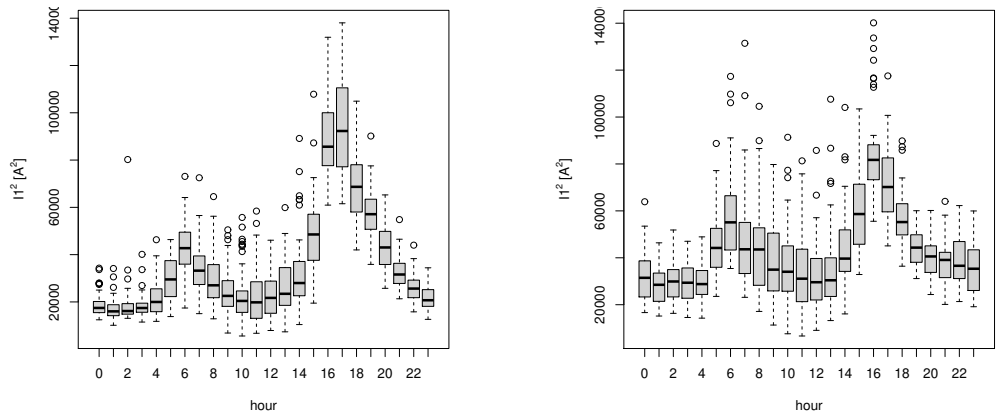

(a) Transformer 1 **(b)** Transformer 2

Figure 2.12 – Current in phase 1.

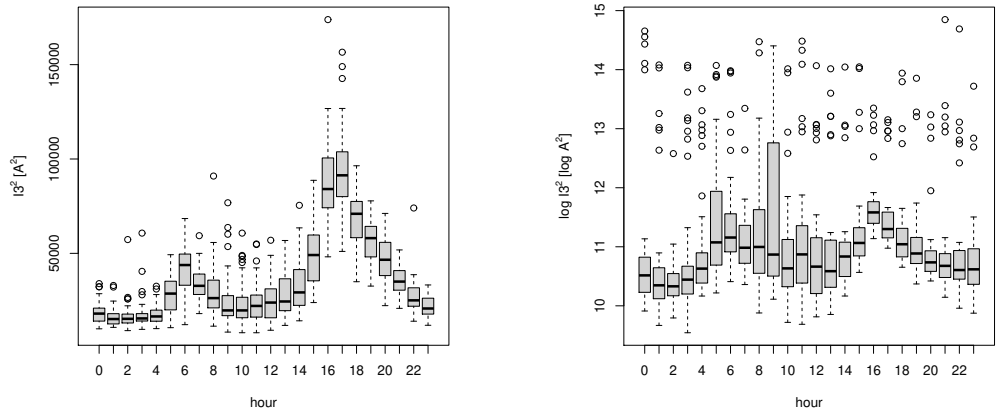

(a) Transformer 1 **(b)** Transformer 2 - Log transformation

Figure 2.13 – Current in phase 3.

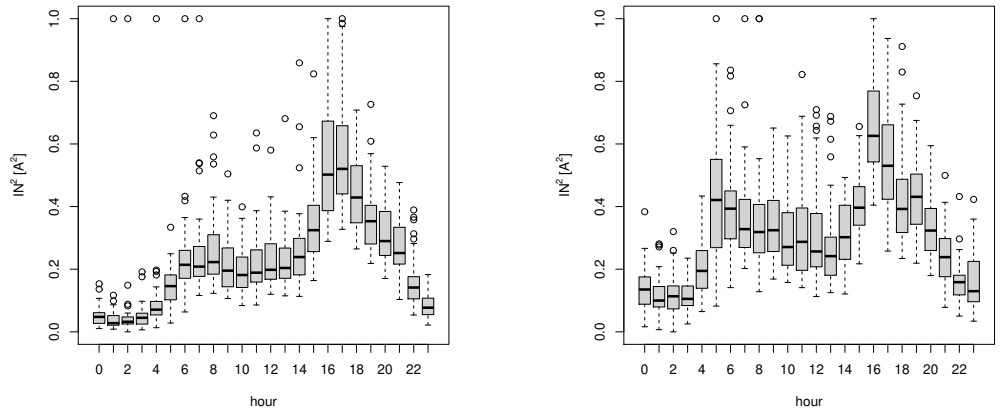

(a) Transformer 1 **(b)** Transformer 2

Figure 2.14 – Harmonics normalized and outliers are removed.

Notice: The comments for phase 2 would be very similar to that of phase 1 hence plots for phase 1 are omitted. Notice further, the resolution of the data is in half hours but for simplicity we report the distributions in hours.

- For phase 1 in figure 2.12, we notice a bimodal distribution. For Transformer 2, the current is stronger for the first spike around hour 6 than for Transformer 1. In general, Transformer 2 has a greater hourly spread than Transformer 1 which we see on the interquartile range and number of outliers.

- For phase 3, we see that Transformer 1 has a distribution quite similar to that of phase 1. For Transformer 2, We use a log transformation to asses the distribution as the signal is very blurred by huge current. It seems that one should handle phase 3 with care or consider excluding it.

- For the neutral current, we see that bimodality is not as obvious as for the other phases. In general, the normalized harmonics is greater for Transformer 2 than 1. We see that the harmonics for Transformer 1 has a very strong peak around hour 17.

2.4 Visual Inspection of Time-Series

In the following, we will inspect two weeks of the series to understand the data type and how inputs from different domains impacts the lid temperature:

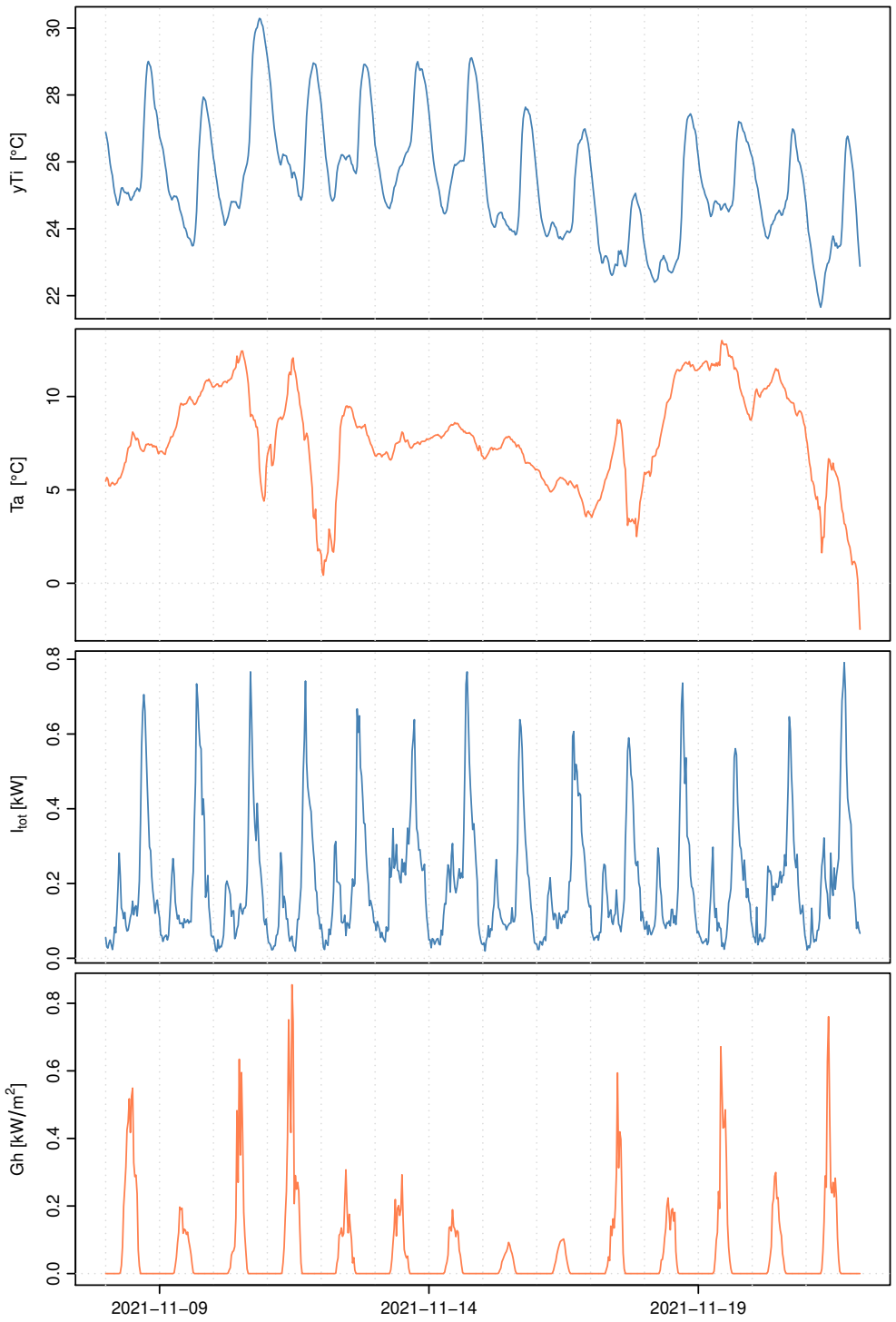

Figure 2.15 – Two weeks of a selection of series for Transformer 1. The vertical lines marks the beginning of a new day.

In fig. 2.15, we observe the following:

1. $yT\ell$ has an obvious daily pattern with peak temperatures close to midnight. The level of the series seems to fluctuate slightly but without any obvious weekly pattern. Note that the series start on a Monday.

2. the ambient temperature, T_a, fluctuates without an obvious pattern. Compare T_a and $yT\ell$ and observe that the level of $yT\ell$ seems to follow the level of the ambient temperature. Consider e.g. the middle part of the series where there is an obvious negative trend in Ta. In the same period, the lid temperature also has a negative trend.

3. I_{tot} has a clear daily pattern with two peaks during the day; in the morning and in the evening. I_{tot} has a weekly pattern with a higher, prolonged morning peak in the weekends.

4. The solar radiation, G_h, has a peak around noon and is zero in the morning, evening, and night hence it would only affect the temperature in a short span of a day.

3 | Transformer 1

3.1 Baseline Model

Before starting on any advanced modeling we set up a simple baseline model, which will be the reference point for all later models. We set up the following time-homogeneous stochastic differential equation of order one:

$$\mathrm{d}T_\ell = \frac{1}{C_\ell}\left[aP_h + b\right]\mathrm{d}t + \sigma \mathrm{d}w \tag{3.1.1}$$

To check how well a model perform, we set up the additional equation based on the actual measurements:

$$yT_\ell = T_\ell + \varepsilon \tag{3.1.2}$$

where ε becomes the residuals for our fitted model.

Intuitively, one would select both a and b strictly greater than zero in eq. (3.1.1). We expect the load-loss to have a positive influence on the change in temperature, hence $a > 0$. Further, we expect that if we only have no-load-loss, then the transformer still releases heat to the system and therefore again influences the lid temperature positively. Forcing a and b to be positive we obtain:

$$a = 5.74 \cdot 10^{-2}, \quad b = 2.06 \cdot 10^{-9} \tag{3.1.3}$$

where both becomes insignificant. This is due to the way we design our baseline model: If both $a > 0$ and $b > 0$, then $\mathrm{d}T_\ell > 0$ at any time. Hence, the estimations of a and b become close to 0 as expected. Thus, our model simply consists of our starting point and some scaled noise. In other words, it becomes a moving-average [4].

The phenomena is illustrated on fig. 3.1. Here the actual half-hourly measures are plotted together with our predictions in the period 01-11 and 07-11 2021. Looking at the 12-step ahead predictions, it becomes evident that our fitted baseline model with a strictly positive a and b is reminiscent to a simple MA-model.

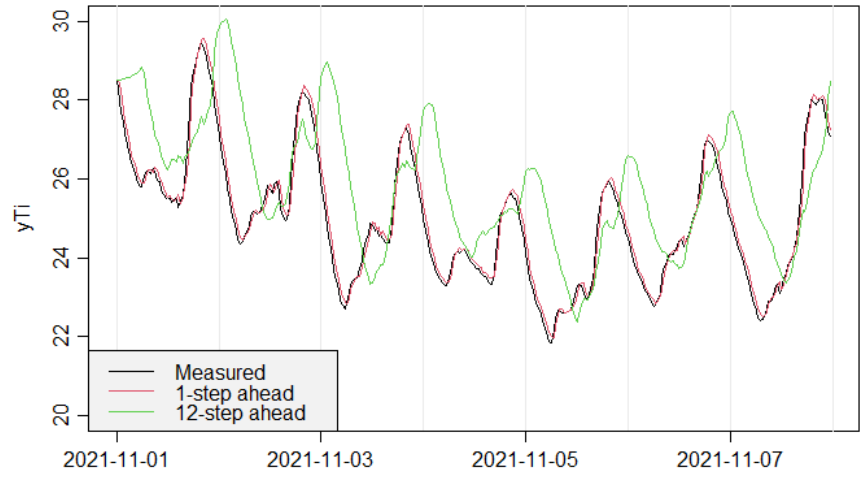

Figure 3.1 – Baseline model with the restrictions $a > 0$ and $b > 0$. The predictions align with a moving average as expected.

Modeling-wise, we relax our parameter b to run in the entire space $\mathbb{R}$. We still demand $a > 0$, since we require an increase in load to have a positive impact on the lid temperature. So based on the physical interpretation above, why is it not a contradiction to relax the parameter b?

Remember, eq. (3.1.1) is a differential equation and not an explicit solution formula for our system. Hence b must be seen relative to our system: When we only have no-load loss, we expect the change in temperature to decrease (or remain constant), as the temperature of the transformer would otherwise be increasing all the time. With $b \in \mathbb{R}$ we get:

$$a = 5.98 \cdot 10^1, \quad b = -1.22 \cdot 10^1$$

hence b is more a mathematical construction or can be seen as the effect of cooling on the lid transformer temperature if we only have no-load loss. The predictions for the same time period as in fig. 3.1:

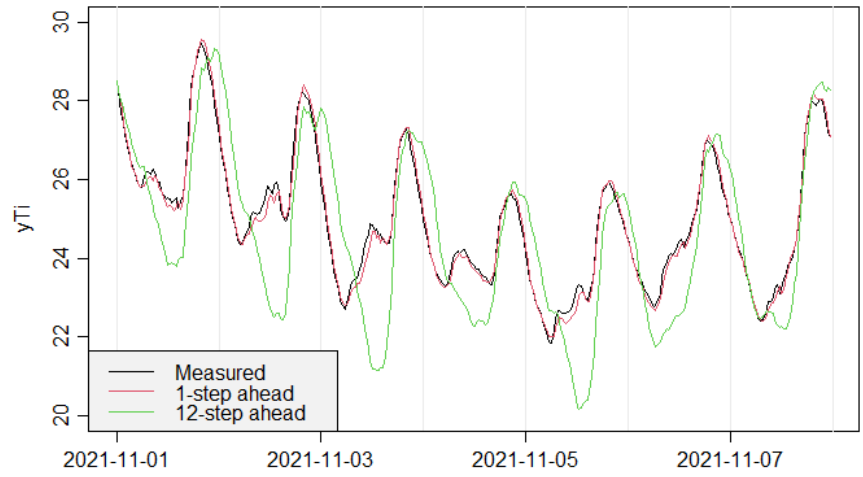

Figure 3.2 – Baseline model with the restrictions $a > 0$ and $b \in \mathbb{R}$. Having included a linear load loss term already seems to improve the n-step ahead predictions.

We are pleased with the results from fig. 3.2 as our baseline model for the transformer lid temperature. For the entire time period [10-11-2021 00:00, 09-12-2021 11:30] with 1440 measurements, we find the residual sum of squares for respectively the 1-step ahead and 12-step ahead:

RSS 1-step	RSS 12-step
35.52	2636.69

Table 3.1 – Baseline results.

To extract additional information from our baseline model the following explanatory plots plots have been produced:

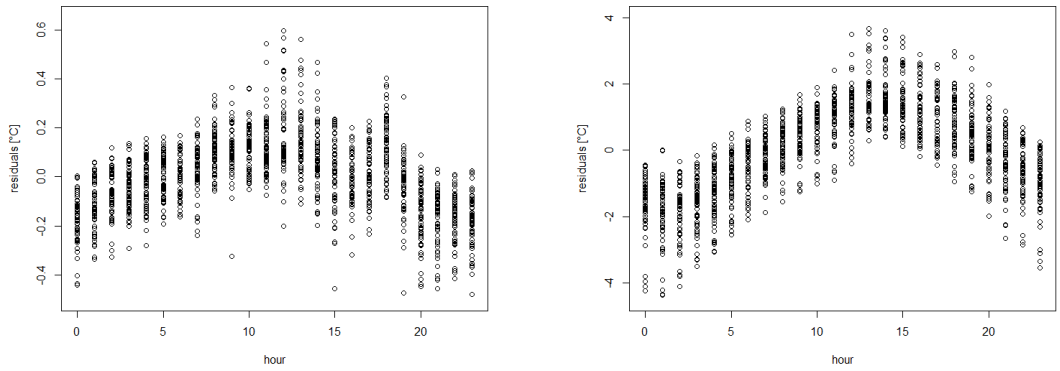

(a) 1-step ahead residuals **(b)** 12-step ahead residuals

Figure 3.3 – Residuals (ε) for the baseline model as a function of time of the day.

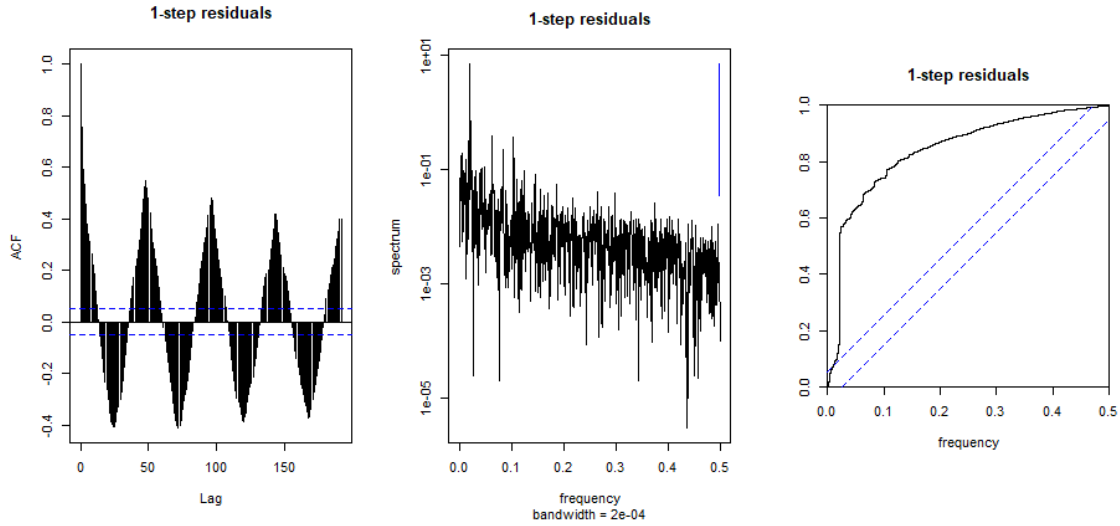

Figure 3.4 – Residual analysis for the baseline model from eq. (3.1.1).

In fig. 3.4, we see that the 1-step ahead residuals are far from white and there is a great deal of systematic variation that the baseline model cannot describe. This aligns with the daily variations seen in fig. 3.3. Further, we see from our 12-step ahead prediction that it seems to scale and shift the residuals.

3.2 One State Models

In the following section, we will model the lid temperature as a one state model. First, we extend the baseline model and include the ambient temperature and other *meteorological variables*. Then we focus on the inclusion of *power variables* as harmonics and rolling means of the power load. With the insights from each domain of variables, we cover findings on how to combine all variables the optimal way.

3.2.1 Meteorological Variables

Ambient Temperature

The transformer is inside a shed without extensive insulation hence we would expect the lid temperature to be affected by the ambient. This relationship, we also see in the data as described in section 2.4. We expect a heat transfer between the ambient temperature and the lid temperature with some resistance, hence we introduce

$$\mathrm{d}T_\ell = \frac{1}{C_\ell}\left[aP_h + b + \frac{1}{R_{\ell a}}\left(T_a - T_\ell\right)\right]\mathrm{d}t + \sigma \mathrm{d}w \tag{3.2.1}$$

This reduces the RSS as seen in table 3.2:

RSS 1-step	RSS 12-step
26.30	1267.99

Table 3.2 – Results with ambient temperature.

Although we have reduced RSS, we still observe that our residuals contain some systematic variance. Thus we will now try extend the model complexity further.

Solar Radiation

Solar radiation will probably heat up the shed, however, this transfer of energy could be highly non-linear. This is both because the sun will hit the shed from different angels during the day and because the transfer of energy could be very non-linear. First, we take the radiation as a linear input to our model, then we make temporal splines to account for shift in angles during the day, and lastly we try to model the radiation with splines to let non-linear dynamics enter linearly.

$$\mathrm{d}T_\ell = \frac{1}{C_\ell}\left[aP_h + b + \frac{1}{R_{\ell a}}\left(T_a - T_\ell\right) + \Psi G v\right]\mathrm{d}t + \sigma \mathrm{d}w \tag{3.2.2}$$

For the linear model Ψ is just some some value $\Psi_{linear} \in \mathbb{R}$.

For the temporal splines Ψ is a sum of 4 splines and parameters $\Psi_{temporal} = \sum_{k=1}^{4} a_k\, bs_k(t)$. The constructed time-based splines, $bs_1(t), bs_2(t), bs_3(t), bs_4(t)$, can be seen in figure 3.5a. They are non-zero from 7-19, otherwise they are 0 because the sun is assumed to only be impact full in that time span. For the radiation based splines, we also construct 4 splines $\Psi_{temporal} = \sum_{k=1}^{4} a_k\, \mathrm{Ghspl}_k(t)$ based on the in-sample data. These data-depended splines can be seen in figure 3.5b. Finally, the results of our model for the different implementations are given in table 3.3 also on the following page.

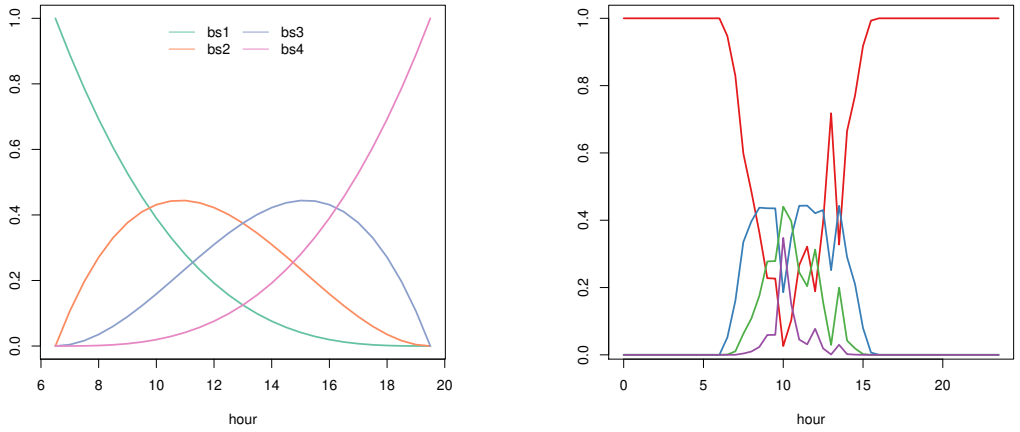

(a) Splines based on time of the day. **(b)** Splines to model non-linear dynamics.

Figure 3.5 – Different approaches to construct splines.

	RSS		BIC
Models	1-step	12-step	1-step
Linearly	21.70	917.73	2571.52
Time-based splines	20.72	852.66	2235.36
Radiation-based splines	21.24	865.22	2393.01

Table 3.3 – RSS and BIC for models with radiation

In table 3.3, we see that the time-based splines are better than the simple linear model, but the radiation-based splines are worse than the time-based splines. The BIC suggests that we should accept the increased complexity of the model with the time-based splines instead of the simpler linear model. In the plots below, we have illustrated the impact of solar radiation on the lid temperature for respectively time-based splines and radiation based-splines. We see that the impact peaks in the morning hours. Further, we see some negative impact for Time-based splines. This suggests that with the current models, our splines are not only covering the impact from the sun.

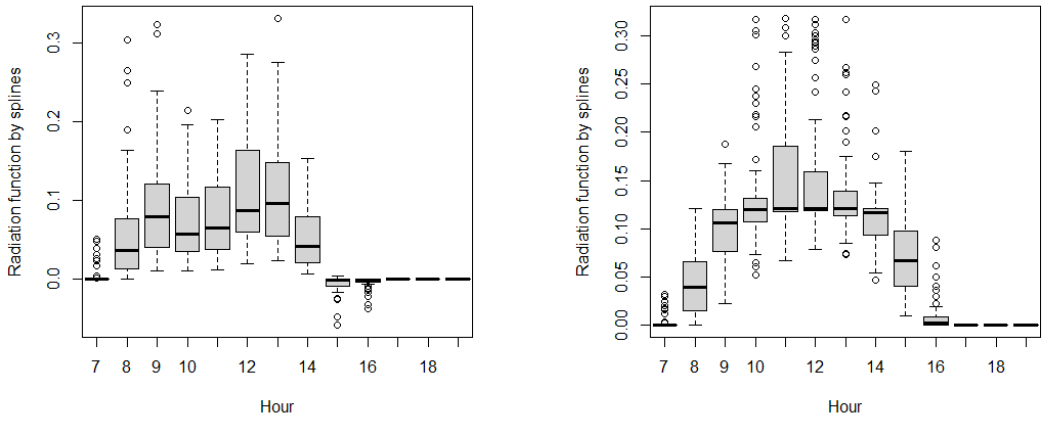

(a) Time-based splines. **(b)** Radiation-based splines.

Figure 3.6 – Solar radiation impact through the different spline approaches.

Wind Speed & Direction

We now try adding information from wind speed and wind direction into our model of the lid temperature. In chapter 2 we uncovered that each wind direction it self was not highly correlated with the transformer's lid temperature. Hence, we apply different methodologies trying adding wind to our models. In this section, we work on improving our current best model: Time-based splines from section 3.2.1.

First, we assume wind direction is not important. This assumption follows follows from fig. 2.7 where we see that most wind is from west i.e. most wind arrive from the same direction and thereby makes the direction less important. We set up the model:

$$\mathrm{d}T_\ell = \frac{1}{C_\ell}\left[aP_h + b + \frac{1}{R_{\ell a}}\left(T_a - T_\ell\right) + \Psi G v + \Phi W s\right]\mathrm{d}t + \sigma \mathrm{d}w \tag{3.2.3}$$

where we have included $WS = \text{windN} + \text{windE} + \text{windS} + \text{windW}$ together with the scaling parameter $\Phi \in \mathbb{R}$.

We obtain:

RSS 1-step	RSS 12-step
19.46	695.06

Table 3.4 – Wind speed results.

With Φ significant. The results from such simple inclusion of wind give rise to an analysis of the impact of wind based on more complex methods. Although most wind arrives from west and decreases the importance of direction, we see from our correlations in section 2.1 that the individual correlations depend highly on the cardinal direction.

Let $\Phi W s$ be the sum $\Phi_1\text{windN} + \Phi_2\text{windE} + \Phi_3\text{windS} + \Phi_4\text{windW}$ in our model eq. (3.2.3), where $\Phi_i, i \in \{1,2,3,4\}$ is the importance parameter for the corresponding cardinal direction. We obtain the following results:

RSS 1-step	RSS 12-step
16.50	368.69

Table 3.5 – Wind speed and cardinal direction results.

together with the parameters:

Parameter	Estimate	P-value
Φ_1	-0.26	$< 2.2e-16$
Φ_2	-0.14	$< 2.2e-16$
Φ_3	-0.17	$< 2.2e-16$
Φ_4	-0.28	$< 2.2e-16$

Table 3.6 – Importance of the different cardinal directions modelling wind speeds.

First of all, we conclude that it is important to include wind direction. When included, it has a negative impact on the lid temperature. Further, we conclude that wind from north or west have the highest impact. Looking again at the windrose fig. 2.7, this indicates that short time intervals of high wind speeds highly influences the entire system including T_ℓ.

Having included the available meteorological variables, we have reduced RSS 1-step by a factor 2 and RSS 12-step by more than a factor 8. We now check, how the residuals are distributed. Have our residuals become white noise?

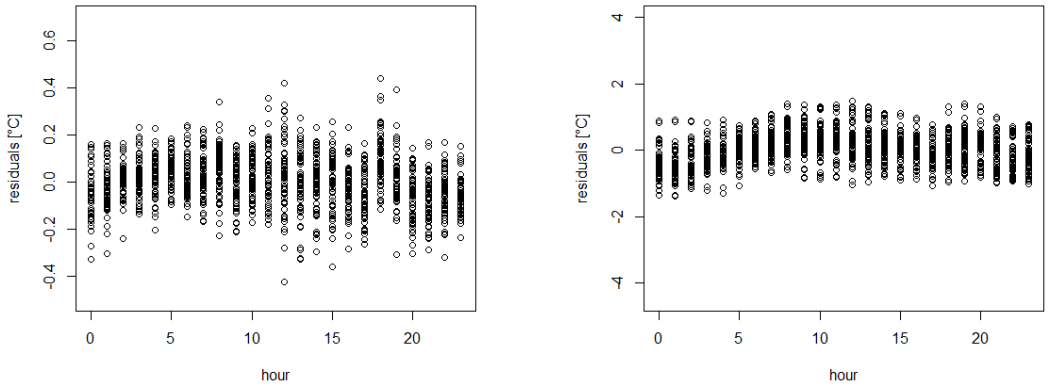

(a) 1-step ahead residuals **(b)** 12-step ahead residuals

Figure 3.7 – Daily variation in residuals (ε) based on eq. (3.2.3) with radiation-based splines and directional wind speeds. We see that the clear patterns from fig. 3.3 have vanished or have been reduced heavily.

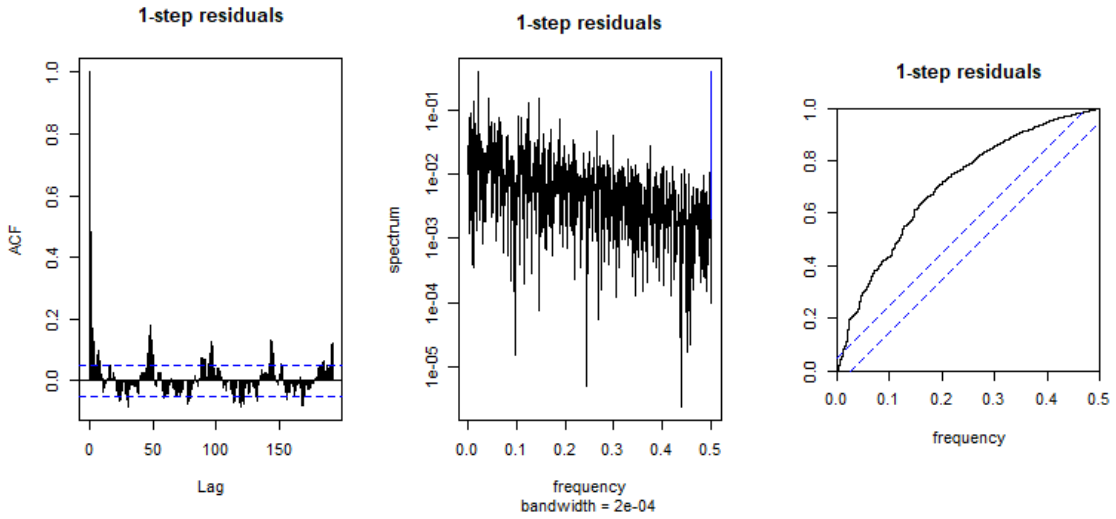

Figure 3.8 – Residual analysis based on eq. (3.2.3) with radiation-based splines and directional wind speeds. We conclude that residuals are generally much cleaner than fig. 3.4 but there are still critical patterns uncovered.

3.2.2 Power Variables

Power Phases

The coils will give rise to coil heating and from Joule's first law we know that the power converted from electrical energy to thermal energy is proportional to the current squared, $P \propto I^2R$. Therefore, we use the sum of the squared currents to get the $P_h = I1^2 + I2^2 + I3^2$ which is also used in the baseline. As a note for this section, we also tried to replace P_h with the sum of the currents $\Psi_h = I1 + I2 + I3$ and the square of the sum $\Psi_h^2 = (I1 + I2 + I3)^2$.

This did not improve the results of our models. When we use the sum of the cubic phases denoted $\rho_h = I1^3 + I2^3 + I3^3$ such that

$$\mathrm{d}T_\ell = \frac{1}{C_\ell}\left[a\rho_h + b\right]\mathrm{d}t + \sigma \mathrm{d}w \tag{3.2.4}$$

then we see a slight improvement in one step predictions.

RSS 1-step	RSS 12-step
33.60	2631.96

Table 3.7 – Results for the cubic phases, ρ_h

We cannot come up with a physical interpretation for cubic phases and it might be an artifact of highly non-linear dynamics that is better captured with the cubic phases.

Harmonics

As described in section 2.3, we will also include harmonics to our model. Here we will also use the square of the current to model the heat contribution from the neural wire.
To see if this makes contribution from the baseline, we consider the one-state model:

$$\mathrm{d}T_\ell = \frac{1}{C_\ell}\left[aP_h + b + c\, IN^2\right]\mathrm{d}t + \sigma \mathrm{d}w \tag{3.2.5}$$

RSS 1-step	RSS 12-step
33.55	2233.69

Table 3.8 – Results with inclusion of harmonics

When we compare this result with the baseline, we see that we only decrease the RSS slightly hence it seems that the harmonics does not add a great deal for Transformer 1.

Rolling Mean

In the data exploration, we see that the lid temperature tends to sustain at relatively high levels if the immediate past loads has been at high levels. Therefore, we include the mean of the last 10 observations as an input to the model. Let $I1_k$ denote the kth observation of the current of phase 1, likewise for $I2_k$, $I3_k$, and introduce $\mu_{10} \in \mathbb{R}^{10}$ as

$$\mu_P^{(10)} = \begin{cases} \frac{1}{k}\sum_{i=1}^{k} I1_k^2 + I2_k^2 + I3_k^2 & \text{for } k \leq 10 \\ \frac{1}{10}\sum_{i=k-10}^{k} I1_k^2 + I2_k^2 + I3_k^2 & \text{for } k > 10 \end{cases} \tag{3.2.6}$$

Likewise we can introduce the mean of the neutral current for the latest 10 data points:

$$\mu_{IN}^{(10)} = \begin{cases} \frac{1}{k}\sum_{i=1}^{k} IN_k^2 & \text{for } k \leq 10 \\ \frac{1}{10}\sum_{i=k-10}^{k} IN_k^2 & \text{for } k > 10 \end{cases} \tag{3.2.7}$$

We try to include the different means to the baseline, one at a time. For $\mu_P^{(10)}$, the model is:

$$\mathrm{d}T_\ell = \frac{1}{C_\ell}\left[aP_h + b + d\mu_P^{(10)}\right]\mathrm{d}t + \sigma \mathrm{d}w \tag{3.2.8}$$

	RSS	
Models	1-step	12-step
Rolling mean with $\mu_P^{(10)}$	35.52	2636.70
Rolling mean with $\mu_{IN}^{(10)}$	35.52	2636.69

Table 3.9 – RSS for the models with rolling mean

In both cases, we barely see improvement, and a, b, C_ℓ, and d turns out insignificant for these models. We conclude that we will not consider the inclusion of rolling means with respect to Transformer 1.

3.2.3 Final Model

Having tried incorporating both environmental and electrical factors, we are left with two clear observations:

- The environmental factors are of high importance reducing our baseline results. The result accounts for both ambient temperature, solar radiation and wind. With these features together we reduce the RSS for our 1-step predictions by a factor 2. Further, for the more complicated 12-step ahead predictions we are above a factor 8 more accurate.
- The electrical factors are well covered by the linear load-loss term in our baseline model. It has been difficult to improve the results significantly by for example including harmonics. One trick is to improve our results is to use the cubic phases $\rho_h = I1^3 + I2^3 + I3^3$.

Combining the two items above, we at first design our final model by:

$$\mathrm{d}T_\ell = \frac{1}{C_\ell}\left[a\rho_h + b + \frac{1}{R_{\ell a}}\left(T_a - T_\ell\right) + \Psi Gv + \Phi Ws\right]\mathrm{d}t + \sigma \mathrm{d}w \tag{3.2.9}$$

with ΨGv denoting time-based splines, while ΦWs is both direction and speed dependent. Keeping the same strict variance we obtain:

RSS 1-step	RSS 12-step
16.15	416.86

Table 3.10 – Final model results.

This final model give us the best 1-step ahead prediction, yet adding only meteorological variables to our baseline model (eq. (3.2.3)) still gives the lowest RSS 12-step ahead. Thus, both models should be considered depending on predicting interests.

We relax the system variance in our final model. Currently, the scale variable $\sigma = 0.0011$. When relaxing the bounds we attain $\sigma = 0.0025$ and the corresponding results:

RSS 1-step	RSS 12-step
16.12	416.30

Table 3.11 – Final model results - relaxed system variance.

We see that relaxing the system variance does not improve our RSS values. This important result suggests that the accuracy of our model is not impacted by our system variance,

thus the physical aspects added in our model seem to carry most information. With the final model, we again plot actual half-hourly measures together with our predictions in the period 01-11 and 07-11 2021. We obtain improvements in the alignment between measures and predictions. Further, the 12-step ahead prediction is no longer shifted with given data.

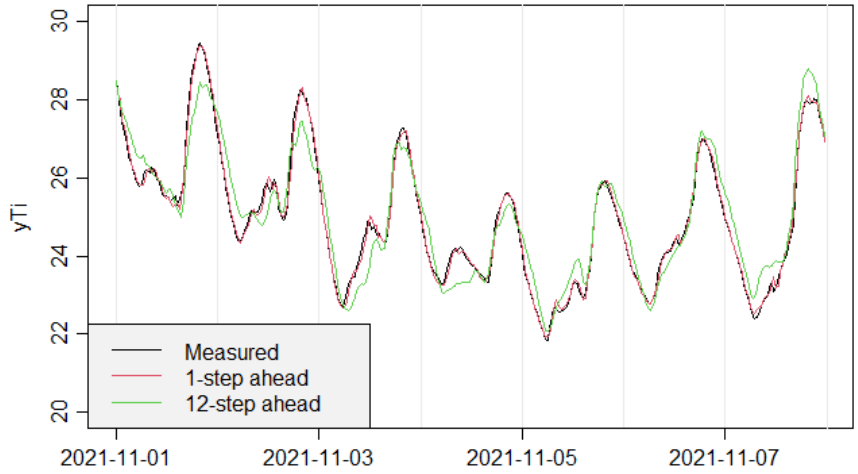

Figure 3.9 – Final model predictions. We see clear improvements for both 1- and 12-step ahead predictions when comparing with fig. 3.2.

In addition to fig. 3.9 we are interested in prediction intervals for our final model. Below, we have included two different ways of making prediction intervals.

At first, assume that we stand at a starting point with yT_ℓ in a specific state. From this starting point all predictions are made without any update hence we would have an increasing prediction interval. A prediction interval based on such method is for our final model seen in fig. 3.10:

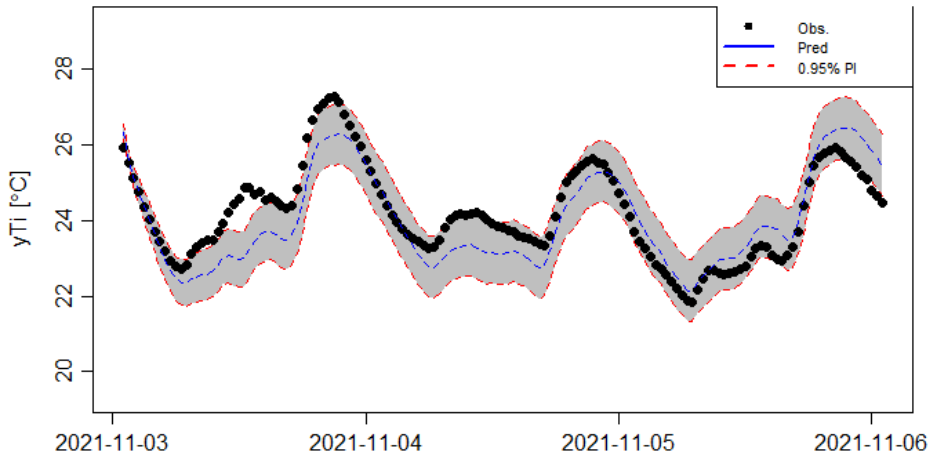

Figure 3.10 – 95% prediction interval plotted from the starting point 03-11-2021 00:00. As expected the interval in general increases as a function of time. *Note that the interval appears small at time of rapid dynamics.*

We can also fix a n-step prediction and update each time increment to make a new n-step step prediction. This method is used for fig. 3.11. Here the interval width at a point is based on a prediction from the n'th observations earlier.

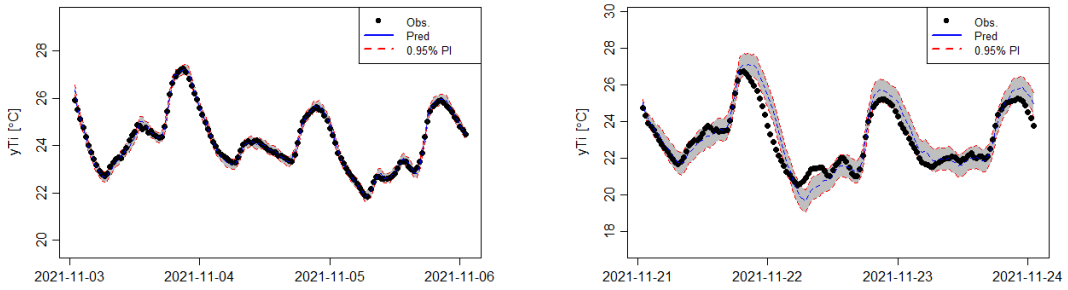

(a) 1-step ahead residuals

(b) 12-step ahead residuals

Figure 3.11 – Observations plotted together with 95% n-step ahead prediction intervals. We see that the 95% intervals cover most of the data points.

In figure 3.11, we see that the 95% prediction interval is very narrow for the 1 step and much wider for the 12 step predictions. The prediction intervals cover most of the points but it seems that it is too optimistic sometimes.

24- and 48- step residuals for our final one state model are reported in Appendix B. Lastly, a table describing the impact of each parameter in the final model is given in Appendix C. The two appendices contain similar results for all final models denoted in this report.

3.2.4 Future Work

We are relatively pleased with the final one-state model based on both RSS values and the plotted predictions. There are still small changes in data that we are not capable of predicting, especially 12-step ahead. In this section, we briefly go through some potential future work in hope of constituting a stimulus for research in such directions.

Include harmonics We have tried adding harmonics to our model but have not found a significant to include the extra heat contribution from the neutral wire. In the modern grid harmonics become more and more critical, hence a study on how to include harmonics to reduce the RSS is of great future interest.

n-step parameters As seen in the analysis above, the best model structure is dependent on how many steps ahead that must be predicted. A study on the importance of different variables as a function of n can give an insight to a general appropriate one-state model.

Stability of solution In this case, a great model leads to a stable solution. We want to be able to find a similar solution when ramping the initial value of a parameter within a short interval of the original value. We have done minor tests on stability, indicating that we have found a local stable solution. Yet, a more strict analysis need to be included to complete such stability study.

3.3 Two State Models

Having analysed models consisting of only one state, we now extend our studies by adding a hidden state. Modelling-wise we set the hidden state to be approximate temperature within the transformer. Due to the importance of such temperature, the actual measures of the hidden state are of interest. In other words, if we design the dynamics for the transformer temperature correctly it becomes possible to give an estimation of such temperature at selected times. These estimations can be used for example designing optimal control.

3.3.1 Extended Baseline

Our first two state model is an extension of our baseline described through section 3.1. It is simply given by:

$$\begin{aligned} \mathrm{d}T_\ell &= \frac{1}{C_\ell}\left[\frac{1}{R_{\ell t}}T_t - T_\ell\right]\mathrm{d}t + \sigma_1 \mathrm{d}w^{(1)} \\ \mathrm{d}T_t &= \left[aP_h + b + \frac{1}{R_{\ell t}}(T_\ell - T_t)\right]\mathrm{d}t + \sigma_2 \mathrm{d}w^{(2)} \\ yT_\ell &= T_\ell + \varepsilon \end{aligned} \tag{3.3.1}$$

The additional hidden state can be understood as some representation of a temperature inside the transformer, T_t. The transfer between T_t and T_ℓ is reduced by the resistance $R_{t\ell}$ and illustrates how the states are connected. Based on eq. (3.3.1) we obtain the following results:

RSS 1-step	RSS 12-step
35.53	2643.22

Table 3.12 – Two state extended baseline results.

As expected the RSS values are equivalent to the results in table 3.1 from our baseline model. Although the structure is more complex by now, we have not in any way exploited the new state. Thus although the complexity of our two state model is higher, the systems eq. (3.1.1) and eq. (3.3.1) are equivalent. With this simple setup we obtain the following statistical representations for our state T_t

$$\mathrm{mean}(T_t) = 24.32, \quad \mathrm{sd}(T_t) = 10.89, \quad \min(T_t) = 10.80, \quad \max(T_t) = 74.35 \tag{3.3.2}$$

with respect to 1-step ahead predictions.

3.3.2 Meteorological Variables

We now turn our focus to include meteorological variables in our two state model. These inclusions force a clear distinction between two states and single state models, since we for the two state models are capable of clarifying the point of attack for respectively meteorological variables and power variables. Similarly to section 3.2.1, we add meteorological variables continuously starting from the inclusion of ambient temperature.

Ambient Temperature

As for one state models, we are interested in incorporating the ambient temperature, since we do not expect the shed to form a closed system due to poor isolation. Now, ambient

impacts do not directly effect our hidden state T_t. Thus, the new system is given by:

$$\begin{aligned} \mathrm{d}T_\ell &= \frac{1}{C_\ell}\left[\frac{1}{R_{\ell t}}(T_t - T_\ell) + \frac{1}{R_{\ell a}}(T_a - T_\ell)\right]\mathrm{d}t + \sigma_1 \mathrm{d}w^{(1)} \\ \mathrm{d}T_t &= \left[aP_h + b + \frac{1}{R_{\ell t}}(T_\ell - T_t)\right]\mathrm{d}t + \sigma_2 \mathrm{d}w^{(2)} \\ yT_\ell &= T_\ell + \varepsilon \end{aligned} \tag{3.3.3}$$

Proceeding with eq. (3.3.3) we obtain the results:

RSS 1-step	RSS 12-step
26.24	1271.28

Table 3.13 – Two states with ambient temperature.

The RSS have become significantly lower and align with the ones found in our one state model. Now our hidden state attains the following statistical representation

$$\text{mean}(T_t) = 52.84, \quad \text{sd}(T_t) = 15.92, \quad \min(T_t) = 29.83, \quad \max(T_t) = 127.76 \tag{3.3.4}$$

with respect to the 1-step ahead predictions.

Solar Radiation

We now add solar radiation to our two-state model. Like for the one-state model, we want to include solar radiation as we expect the amount of radiation on the outside of the shed to have a direct impact on the lid temperature T_ℓ. Our new two state model is given below:

$$\begin{aligned} \mathrm{d}T_\ell &= \frac{1}{C_\ell}\left[\frac{1}{R_{\ell t}}(T_t - T_\ell) + \frac{1}{R_{\ell a}}(T_a - T_\ell) + \Psi G v\right]\mathrm{d}t + \sigma_1 \mathrm{d}w^{(1)} \\ \mathrm{d}T_t &= \left[aP_h + b + \frac{1}{R_{\ell t}}(T_\ell - T_t)\right]\mathrm{d}t + \sigma_2 \mathrm{d}w^{(2)} \\ yT_\ell &= T_\ell + \varepsilon \end{aligned} \tag{3.3.5}$$

As we expect the impact to be non-linear, we introduce the same 3 ways of modelling solar radiation as for the one-state model. Again, to attain some physical understanding of our spline terms, we constrain the amount of splines to be exactly 4 for both time-based and radiation-based models. With the splines illustrated in fig. 3.5a and fig. 3.5b, we get:

	RSS		**BIC**
Models	1-step	12-step	1-step
Linearly	21.66	920.46	2571.52
Time-based splines	20.69	855.82	2245.487
Radiation-based splines	21.20	867.82	2400.68

Table 3.14 – RSS and BIC for two-state models with radiation.

The results are similar to the one-state results. We again select to continue with the time-based splines as it gives the best physical interpretation and the lowest RSS values. Including solar radiation, the hidden state attains the following statistical representation:

$$\text{mean}(T_t) = 42.21, \quad \text{sd}(T_t) = 14.31, \quad \min(T_t) = 22.57, \quad \max(T_t) = 109.48 \tag{3.3.6}$$

Wind Speed & Direction

Following on the solar radiation results, we include the impact wind speed and direction with the term ΦWs:.

$$\begin{aligned} \mathrm{d}T_\ell &= \frac{1}{C_\ell}\left[\frac{1}{R_{\ell t}}(T_t - T_\ell) + \frac{1}{R_{\ell a}}(T_a - T_\ell) + \Psi G v + \Phi W s\right]\mathrm{d}t + \sigma_1 \mathrm{d}w^{(1)} \\ \mathrm{d}T_t &= \left[aP_h + b + \frac{1}{R_{\ell t}}(T_\ell - T_t)\right]\mathrm{d}t + \sigma_2 \mathrm{d}w^{(2)} \\ yT_\ell &= T_\ell + \varepsilon \end{aligned} \tag{3.3.7}$$

Like for the one-state model we try defining wind both with and without cardinal wind direction as a parameter. We obtain:

	RSS	
Models	1-step	12-step
Wind speed only	17.14	527.51
Wind speed and direction	16.38	371.36

Table 3.15 – RSS for the models including wind impact.

Now our two-state 'wind speed only' model outperforms the corresponding one-state model both for 1- and 12-step ahead predictions. With respect to wind speed and cardinal wind direction the results are similar to the one-state model. We see a small improvement in 1-step prediction, while 12-step predictions become a bit worse. Adding cardinal wind direction as a parameter the residuals of our model fit become:

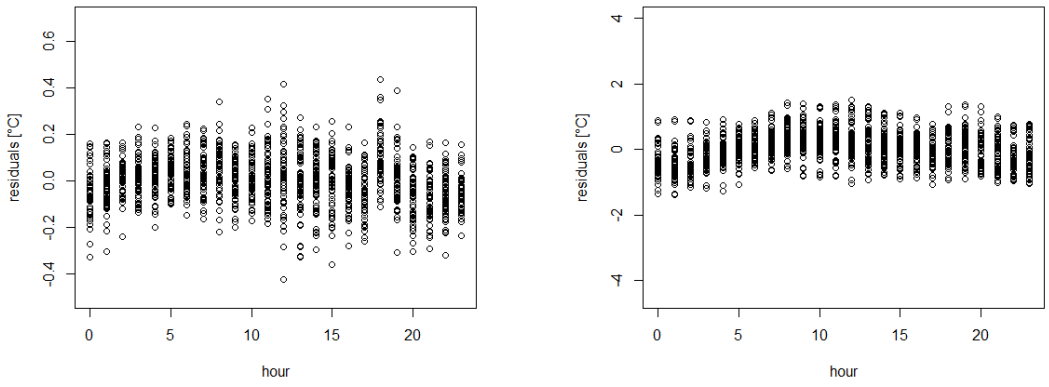

(a) 1-step ahead residuals **(b)** 12-step ahead residuals

Figure 3.12 – The residuals do not contain the same strong patterns as our general baseline model. Although, we seem to find id difficult to model the load peaks around 18-19 o'clock. We try handle the critical residuals in the following section by including power variables.

Finally the new statistical representation of our hidden state is given by:

$$\mathrm{mean}(T_t) = 84.00, \quad \mathrm{sd}(T_t) = 21.65, \quad \min(T_t) = 48.20, \quad \max(T_t) = 186.74 \tag{3.3.8}$$

As documented, the hidden state T_t experiences a high increase in temperature. The results are expected, since wind provided a negative impact on T_ℓ forcing T_t to attain higher values to accurately approximate T_ℓ. The opposite trend in T_t temperatures was experienced including solar radiation caused by the suns positive impact on T_ℓ.

3.3.3 Power Variables

Contrary to the one-state model, we try adding the power parameters directly to our optimal meteorological model. We add directly, as we would like to see the influence of adding information to the hidden state in a two-state model. This is done through the three subsections below:

Power Phases

First we try interchange P_h with Ψ_h, Ψ_h^2 and ρ_h. Their respective definitions are given in section 3.2.2. Although Joule's first law tells that the thermal energy is proportional to current squared, we are not sure that it modelling wise is the best approximation. The results for our different load-loss functions substituted with P_h in eq. (3.3.7) become:

	RSS	
Models	1-step	12-step
$\Phi_h = I1 + I2 + I3$	19.62	420.57
$\Phi_h^2 = (I1 + I2 + I3)^2$	16.27	369.80
$\rho_h = I1^3 + I2^3 + I3^3$	16.10	416.77

Table 3.16 – RSS for the different power phases dependent functions

Remark, multiple power phase functions seem fitting dependent on what to predict. Contrary to one-state models, using Φ_h^2 improves both 1- and 12-step predictions. By the significant lower 1-step score from the cubic expression ρ_h, we decide to select it instead of P_h in future two-state Transformer 1 models. Substituting P_h with ρ_h leaves us with the following statistical representation of our hidden state T_t:

$$\text{mean}(T_t) = 51.54, \quad \text{sd}(T_t) = 10.75, \quad \min(T_t) = 38.35, \quad \max(T_t) = 116.00 \tag{3.3.9}$$

Harmonics

Based on the theory from section 2.3, we try including the effect of harmonics to our two-state model. Again, we use the square of the current to model heat contribution from the neutral wire.

$$\begin{aligned} \mathrm{d}T_\ell &= \frac{1}{C_\ell}\left[\frac{1}{R_{\ell t}}(T_t - T_\ell) + \frac{1}{R_{\ell a}}(T_a - T_\ell) + \Psi G v + \Phi W s\right]\mathrm{d}t + \sigma_1 \mathrm{d}w^{(1)} \\ \mathrm{d}T_t &= \left[a\rho_h + b + c\,IN^2 + \frac{1}{R_{\ell t}}(T_\ell - T_t)\right]\mathrm{d}t + \sigma_2 \mathrm{d}w^{(2)} \\ yT_\ell &= T_\ell + \varepsilon \end{aligned} \tag{3.3.10}$$

In the table below we see, that including neutral current squared only provides a small reduce in RSS-values:

RSS 1-step	RSS 12-step
16.08	413.30

Table 3.17 – Two-state model based on eq. (3.3.10)

We will proceed with neutral current squared include as the parameter c is significant for our model. Now the statistical representation of T_t becomes:

$$\text{mean}(T_t) = 50.95, \quad \text{sd}(T_t) = 10.46, \quad \min(T_t) = 38.01, \quad \max(T_t) = 113.39 \tag{3.3.11}$$

Rolling Mean

A transformer has an inertia constraining the heat transfer. Hence, we suspect that T_t sustains at relatively high levels if the immediate past loads has been at high levels. Modelling-wise we set up a rolling mean similarly to section 3.2.2. Including a rolling mean with respect to neutral current in our current best model give us the structure:

$$\begin{aligned} \mathrm{d}T_\ell &= \frac{1}{C_\ell}\left[\frac{1}{R_{\ell t}}(T_t - T_\ell) + \frac{1}{R_{\ell a}}(T_a - T_\ell) + \Psi G v + \Phi W s\right]\mathrm{d}t + \sigma_1 \mathrm{d}w^{(1)} \\ \mathrm{d}T_t &= \left[a\rho_h + b + c\,IN^2 + d\,\mu_{IN}^{(20)} + \frac{1}{R_{\ell t}}(T_\ell - T_t)\right]\mathrm{d}t + \sigma_2 \mathrm{d}w^{(2)} \\ yT_\ell &= T_\ell + \varepsilon \end{aligned} \tag{3.3.12}$$

The corresponding results and a statistical representation of the hidden state are found:

RSS 1-step	RSS 12-step
15.99	415.16

Table 3.18 – Two-state model based on eq. (3.3.12)

$$\mathrm{mean}(T_t) = 79.19, \quad \mathrm{sd}(T_t) = 20.88, \quad \min(T_t) = 47.86, \quad \max(T_t) = 206.28 \tag{3.3.13}$$

Notice that the state values seem very high, hence the hidden state probably does not represent exactly the temperature within the transformer..

3.3.4 Final Model

For the best two state model with respect to Transformer 1 we suggest to use eq. (3.3.10) with ΨGv implemented with based splines and ΦWs dependent on both speed and direction. There are two main reasons behind the choice:

- The RSS 1- and 12- step are both relatively close to the minimum values achieved. Hence the model seem to be capable of predicting the correct level for T_ℓ both 30 minutes after the current state and 6 hours afterwards.
- The statistical representation of T_t matches the temperature one could expect within a transformer eq. (3.3.11). An analysis of the hidden state is given on the next page.

After relaxing the system variance which again leads to small reductions in RSS, we start looking at the residuals from our final model. The daily variation is shown below:

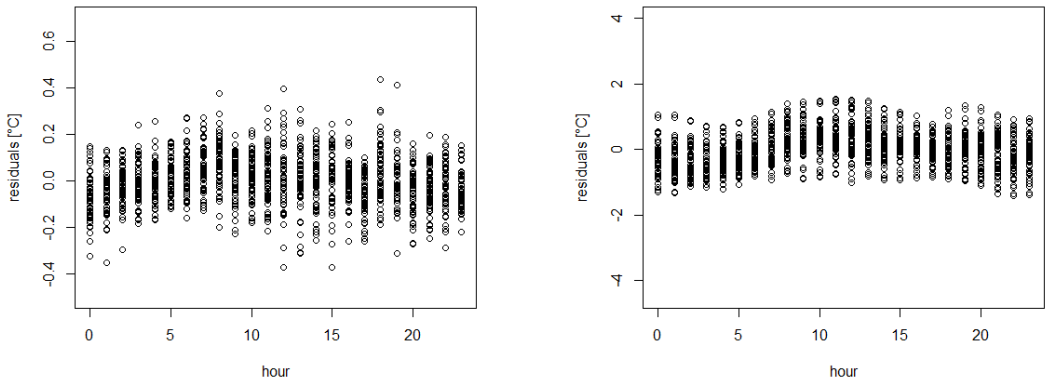

(a) 1-step ahead residuals **(b)** 12-step ahead residuals

Figure 3.13 – The daily variations in residuals are similar to the ones from fig. 3.12

Continuing analysing residuals, we have produced the following triplets of plots based on 1-step ahead prediction residuals:

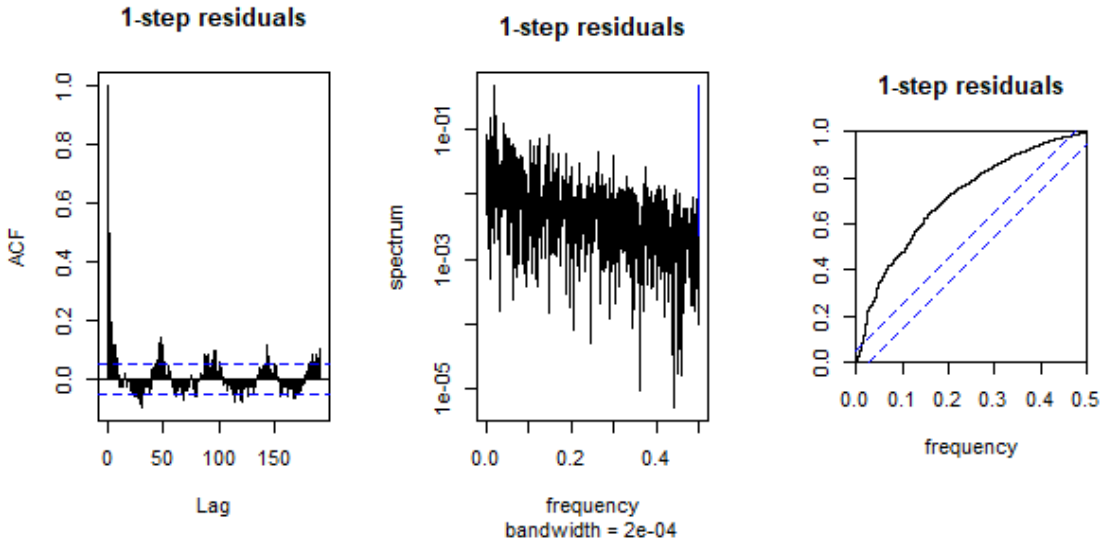

Figure 3.14 – The auto-correlation function shows that there are daily variation also with respect to 1-step residuals, that we are not able to model. This align with the results from the two frequency dependent plots showing that our residuals are not entirely white noise.

The residuals are in general similar to the results using only one-state. For ideas to force different results the reader is referred to section 3.3.5. Instead, we will now look at the values our hidden state attains when fitting eq. (3.3.10).

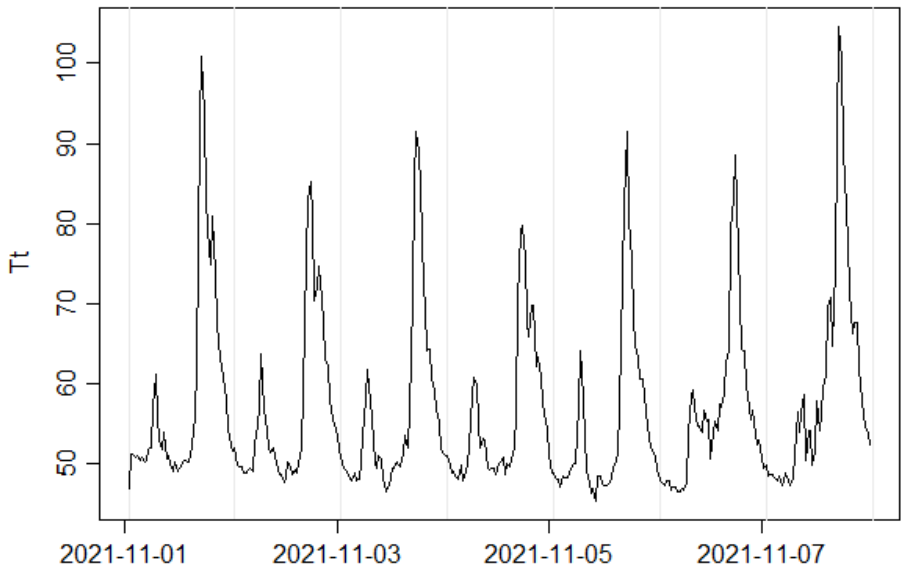

Figure 3.15 – The hidden state plotted as a function of time. Here we have illustrated the state during the first week of November. The general patterns are similar to the graph of I_{tot} from fig. 2.15. We see that the indirect effects from environmental factors also play a role for the state of T_t. We are pleased with the hidden state as the temperatures seem reasonable and as well as the daily behavior.

3.3.5 Future Work

An additional state could be added to the one-state system in many different ways. Here, we have chosen a hidden together with the interpretation of the state to model the temperature. In this brief section we will discuss different model set ups and illustrate some pros and cons. Based on the discussion, we include an entirely new dynamic system for Transformer 1 for which additional work could be of interest.

By now, the primary focus has been to include the hidden state correctly such that it can be understood as some temperature within the transformer. Hence, our current model structures are build similarly to the one-state models. The similar structures imply similar residuals patterns. Below, we suggest a couple of designs to force drastically different results for two-state models:

Interplay between states A way to force different model structures is to change the interplay between the two states. Here, we could a non-linear interference. Finally, it is also an idea to work on specific state variances to adapt to the importance of the state's physical interpretations.

Different second states Another way to force different model structures is to add a different second state, where observations are available. This way requires a more extensive analysis but can provide important information of the system behaviours and heat transfers. We start the analysis below adding T_{top} as the second state.

Two-state $\mathbf{T_{top}}$

In this short section, we add T_{top} as the second state. We add T_{top} since we have observations given for the variable. Now T_ℓ becomes the state where electrical factors impact, while T_{top} is positioned close to the roof of the shed. Hence, it is more sensitive to environmental factors. The chosen model eq. (3.3.14) is designed based on our current best two-state model (when having a hidden second state instead).

$$
\begin{aligned}
\mathrm{d}T_{\text{top}} &= \frac{1}{C_{\text{top}}}\left[\frac{1}{R_{\ell\text{top}}}(T_\ell - T_{\text{top}}) + \frac{1}{R_{\text{top}\,a}}(T_a - T_{\text{top}}) + \Psi G v + \Phi W s\right]\mathrm{d}t + \sigma_1 \mathrm{d}w^{(1)} \\
\mathrm{d}T_\ell &= \frac{1}{C_\ell}\left[a\rho_h + b + c\,I N^2 + \frac{1}{R_{\ell\text{top}}}(T_{\text{top}} - T_\ell)\right]\mathrm{d}t + \sigma_2 \mathrm{d}w^{(2)} \\
yT_\ell &= T_\ell + \varepsilon^{(1)} \\
yT_{\text{top}} &= T_{\text{top}} + \varepsilon^{(2)}
\end{aligned}
\tag{3.3.14}
$$

Optimizing with respect to both known states we find for relaxed system variance that:

RSS 1-step	RSS 12-step
15.93	940.96

Table 3.19 – T_ℓ

RSS 1-step	RSS 12-step
88.68	3951.70

Table 3.20 – T_{top}

Table 3.21 – Residuals for both states based on eq. (3.3.14).

with all parameters being significant to include. The one-step results are relative impressive, while 12 step ahead prediction forces large residuals.

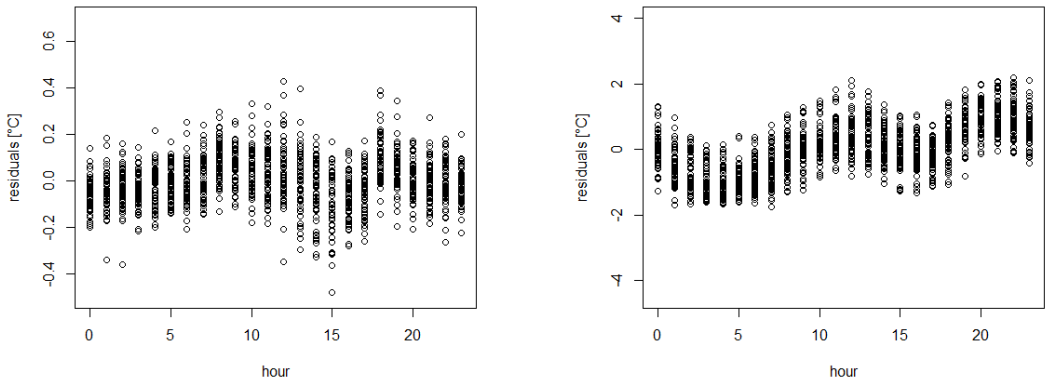

(a) 1-step ahead residuals **(b)** 12-step ahead residuals

Figure 3.16 – The daily variations in residuals for eq. (3.3.14). The 1-step prediction residuals are relatively close to white noise. There is some issue around 15 o'clock. Now the 12-step prediction residuals seem to have hidden patterns which we have not been able to correct.

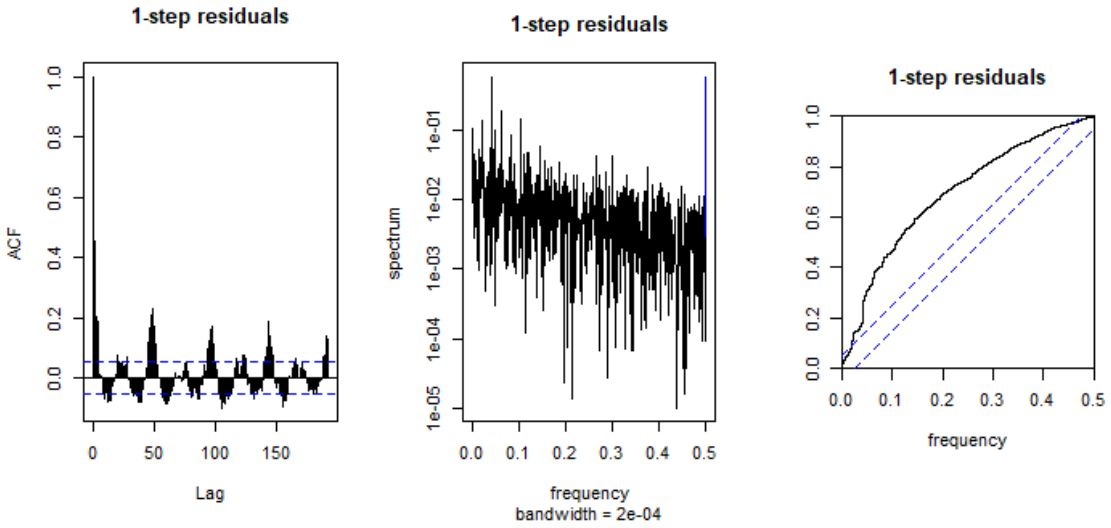

Figure 3.17 – The auto-correlation function shows that there are daily variation again with respect to 1-step residuals. The results from the two frequency dependent plots also adds weight to the fact that our residuals are not entirely white noise.

We try adding direct impact of ambient temperature for T_ℓ as well. The updated system becomes:

$$\begin{aligned}
\mathrm{d}T_{\text{top}} &= \frac{1}{C_{\text{top}}}\left[\frac{1}{R_{\ell\text{top}}}(T_\ell - T_{\text{top}}) + \frac{1}{R_{\text{top}\,a}}(T_a - T_{\text{top}}) + \Psi G v + \Phi W s\right]\mathrm{d}t + \sigma_1 \mathrm{d}w^{(1)} \\
\mathrm{d}T_\ell &= \frac{1}{C_\ell}\left[a\rho_h + b + c\,IN^2 + \frac{1}{R_{\ell\text{top}}}(T_{\text{top}} - T_\ell) + \frac{1}{R_{\ell\,a}}(T_a - T_\ell)\right]\mathrm{d}t + \sigma_2 \mathrm{d}w^{(2)} \\
yT_\ell &= T_\ell + \varepsilon^{(1)} \\
yT_{\text{top}} &= T_{\text{top}} + \varepsilon^{(2)}
\end{aligned} \tag{3.3.15}$$

We did not find better results adding ambient impact for both. In fact both wind and solar became insignificant. We encourage readers to continue studying such two-states.

4 | Transformer 2

In this chapter, we will briefly cover findings for Transformer 2 with focus on where the results differs from the results obtained for Transformer 1. It can be read in the following that phase 3 of the load in the provided data set was corrupted. We were provided with a new corrected data set one day prior to the deadline and hence we have only discussed this data set briefly in appendix A. Thus, the reader is referred to appendix A for a non-disturbed data analysis of Transformer 2.

4.1 Baseline Model

In section 2.3.3, we notice that phase 3 has signal with many outliers and very high values. Therefore, we speculate that it should be excluded such that the P_h of the baseline in equation 3.1.1 is modified to be $I1^2 + I2^2$ normalized. When we do this, we see a great improvement as seen in table 4.1. Therefore, we will only use phase 1 and 2 for all results with respect to Transformer 2.

	RSS	
Models	1-step	12-step
Baseline	343.06	16030.27
Baseline Phase 1 & 2	152.38	9887.66

Table 4.1 – RSS for the baseline models

4.2 One State Models

4.2.1 Meteorological Variables

Ambient Temperature

First we add ambient temperature as it works really well for Transformer 1. In table 4.2, we see that this is also very important for Transformer 2 with a huge decrease in the RSS.

RSS 1-step	RSS 12-step
73.035	1565.33

Table 4.2 – Results with ambient temperature for Transformer 2.

Just by including ambient temperature in our one state model we reduce RSS 1-step by a factor 2, while the RSS 12 step is reduced by a factor 6. With the impressive reduction, we are now interested in adding other meteorological variables.

Solar Radiation

For the solar radiation it seems that time-based splines outperform other implementations. Radiation-based splines are great on 1-step predictions but is in general outperformed.

	RSS		BIC
Models	1-step	12-step	1-step
Linearly	67.94	1371.52	13514.16
Time-based splines	65.13	1260.41	13034.38
Radiation-based splines	64.48	1291.37	13187.9

Table 4.3 – RSS and BIC for models with radiation.

Wind Speed & Direction

The results in the table below are surprising: We see that wind speed reduces the RSS scores for 1- and 12-step, while adding direction makes the optimization perform worse. This error could be caused by optimizing disturbances, so we continue to try adding direction as well.

	RSS	
Models	1-step	12-step
Wind speed only	56.10	826.53
Wind speed and direction.	131.01	7442.35

Table 4.4 – RSS including wind impacts.

4.2.2 Power Variables

Power Phases

We only use phase 1 and 2 for Transformer 2. However, it would still be interesting to use the sum of the cubic phases hence we use $\rho_h = I1^3 + I2^3$ phases:

RSS 1-step	RSS 12-step
141.01	9629.94

Table 4.5 – Results when we use $\rho_h = I1^3 + I2^3$.

Here we again see an improvement from the baseline.

Harmonics

When we include the harmonics as in equation 3.2.5, we see only a slight decrease:

RSS 1-step	RSS 12-step
149.14	9252.28

Table 4.6 – Results with inclusion of harmonics.

Rolling Mean

Consult section 3.2.2, to see the equations and definitions of the rolling means. Note that the $\mu_p^{(10)}$ is also only based on the phase 1 and 2. In both cases, the coefficient in for the included rolling means is insignificant and the RSS values are do not decrease.

	RSS	
Models	1-step	12-step
Rolling mean with $\mu_P^{(10)}$	152.38	9887.68
Rolling mean with $\mu_{IN}^{(10)}$	152.38	9887.78

Table 4.7 – RSS for the models with rolling mean.

4.2.3 Final Model

The inputs to include are very similar to that of Transformer 1. This time we should exclude phase 3 and include the ambient temperature, the solar radiation splines, the wind speed & direction and finally the neutral current. We find that the best one state model for Transformer 2 performs:

RSS 1-step	RSS 12-step
52.814	775.493

Table 4.8 – Results for the final one state model for Transformer 2.

We have managed to reduce the RSS significantly compared to the simpler baseline model. In general, we see that Transformer 2 results are sufficiently worse than for Transformer 1.

4.3 Two State Models

4.3.1 Extended Baseline

As for Transformer 1, we start our two state modelling by an extension of our baseline model. With our set optimization constraints we were not able to find a result for such model for Transformer 2. This is due to a singular correlation matrix after a large number of CTSM iteration. Testing different optimization constraints did not do the trick and we are left without results for the extended baseline. The tests have been done based on expected final parameter values (aligned with T2 one state baseline model parameters).

4.3.2 Meteorological Variables

Ambient Temperature

We continue by adding ambient temperature to our model. We still are not capable of attaining clean results. Now we are faced with the warning: 'Using a diagonal' leading to the following critical RSS-scores:

RSS 1-step	RSS 12-step
1807.59	1958.32

Table 4.9 – Results including ambient temperature.

Solar Radiation

For the solar radiation it seems that the time-based splines again outperform the other ways of implementing the solar radiation as it attain the lowest BIC value. Note for the two-state model, radiation-based splines also gives a great fit. Hence, we proceed with radiation-based splines modeling solar radiation.

	RSS		BIC
Models	1-step	12-step	1-step
Linearly	67.80	1374.16	23709.08
Time-based splines	64.54	1285.13	13034.38
Radiation-based splines	63.60	1310.93	13054.81

Table 4.10 – RSS and BIC for models with radiation.

The statistical representation of our hidden state becomes:

$$\text{mean}(T_t) = 339.62, \quad \text{sd}(T_t) = 113.70, \quad \min(T_t) = 44.98, \quad \max(T_t) = 840.85 \tag{4.3.1}$$

Wind Speed & Direction

Now, both wind speed & direction lower the RSS scores for 1- and 12-step. Having included all environmental factors we find the lowest RSS score to be 52.54.

	RSS	
Models	1-step	12-step
Wind speed only	55.09	848.84
Wind speed and direction	52.54	669.89

Table 4.11 – RSS including wind impacts.

With the addition of wind, the statistical representation of our hidden state becomes:

$$\text{mean}(T_t) = 185.07, \quad \text{sd}(T_t) = 47.72, \quad \min(T_t) = 46.91, \quad \max(T_t) = 391.15 \tag{4.3.2}$$

4.3.3 Power Variables

Like for our two state models for Transformer 1, we add power variables onto the best current system with environmental variables included. The performances are shown below:

Power Phases

With only phase 1 and 2 in use it is still of interest to check how to implement the heat loss from current in our system. We have tried the 3 different methods from the table below:

	RSS	
Models	1-step	12-step
$\Phi_h = I1 + I2$	64.88	783.98
$\Phi_h^2 = (I1 + I2)^2$	52.36	662.81
$\rho_h = I1^3 + I2^3$	52.59	784.26

Table 4.12 – RSS for the different power phases dependent functions.

It becomes evident that $\Phi_h^2 = (I1+I2)^2$ is our optimal expression. The results are different from two state Transformer 1 models and indicate that the missing information from $I3$ effects our modelling.

The statistical representation of our hidden state becomes:

$$\text{mean}(T_t) = 178.46, \quad \text{sd}(T_t) = 45.61, \quad \min(T_t) = 46.65, \quad \max(T_t) = 375.90 \tag{4.3.3}$$

Harmonics

Continuing with $\Phi_h^2 = (I1 + I2)^2$ instead of P_h we see that adding a term with neutral current squared (representing harmonics) does reduce RSS but only marginally:

RSS 1-step	RSS 12-step
51.71	653.36

Table 4.13 – Results with inclusion of harmonics.

The statistical representation of our hidden state becomes:

$$\text{mean}(T_t) = 137.10, \quad \text{sd}(T_t) = 33.06, \quad \min(T_t) = 46.77, \quad \max(T_t) = 278.40 \tag{4.3.4}$$

Rolling Mean

Finally we include rolling mean for our two state model as well to incorporate transformer inertia. As for one state modelling this does not improve our best fit:

RSS 1-step	RSS 12-step
51.75	654.51

Table 4.14 – Two-state model based on rolling mean $\mu_{IN}^{(10)}$.

The statistical representation of our hidden state becomes:

$$\text{mean}(T_t) = 140.58, \quad \text{sd}(T_t) = 34.06, \quad \min(T_t) = 46.75, \quad \max(T_t) = 286.14 \tag{4.3.5}$$

4.3.4 Final Model

For two state models Transformer 2, our best fit is fund by adding all environmental factors: Ambient temperature, time-based splines solar radiation, wind speed and wind direction. Further one should consider using combination of terms when modelling heat loss as a function of current. We suggest Φ_h^2. Adding a term with the neutral current squared also gives valuable information emphasising some kind of impact from harmonics. The RSS scores for such model are found in table 4.13.

For Transformer 2, we observe that our hidden state attains high values. Thus, in general the statistical representation of our hidden state do not align with a statistical representation of actual temperatures within a transformer.

For our final model we find the most fitting statistical representation, but the values are still to high. The abnormal hidden state for Transformer 2 elucidates that we have not been able to separate environmental factors and electrical factors properly. We expect this conclusion to causing the general higher RSS scores for Transformer 2.

We have decided not to try improving our Transformer 2 model further based on the current input data. This is due to the lack of non-disturbed measurements for $I3$. As $I3$ in general is available without heavy noise, a more complex Transformer 2 model would then potentially not perform better when exact measures of $I3$ is available again.

5 | Conclusion

The transformer temperature is affected by power inputs and environmental factors and it is important how the inputs are presented to the CTSM-model and how the inputs are combined. The current and sum of the squared phases served as a onestate baseline model with an 1-step RSS of 35.52 for Transformer 1. The most essential environmental variables is the ambient temperature. We find that time-based splines are the best option to implement solar radiation and wind is best implemented using the cardinal direction and the inclusion of all of them gives a 1-step RSS of 16.50 for Transformer 1. Inclusion of the neutral phase and rolling means of power variables give minor improvements. The two state models has the same performance but when we introduce the second hidden state it serves as a nice interpretation of the temperature dynamics in the transformer.

Transformer 2 exhibits more complex dynamics hence the model performance is in general inferior to that of Transformer 1. The signal in phase 3 was initially blurred hence excluded and the baseline only included phase 1 and 2 with a 12-step RSS on 9887.66. In this case, the final one state model has 12-step RSS on 775.49; however the two state model could bring this down to 654.51 hence the added state improves the model. Using this model the available tools in CTSM-R, we can understand some representation of heat dynamics through the hidden state. It is very interesting to follow how the dynamics shifts when new variables are introduced where the temperature of the hidden state change dramatically depending on the way the model is constructed.

6 | Appendix

Appendix A

Luckily, we were provided with a new data set for transformer 2 where phase 3 in the load signal was not corrupted the day before hand-in we were. Due to the late arrival of the data set we were not able to redo all the models for transformer 2. Instead, we will compare the baseline and final model with one state for Transformer 2.

	RSS	
Models	1-step	12-step
Baseline with phase 1 and 2	343.06	16030.27
Baseline with phase 1, 2 and 3	160.91	10628.91

Table 6.1 – RSS for the baseline.

	RSS	
Models	1-step	12-step
Final model with phase 1 and 2	52.814	775.493
Final model with phase 1, 2 and 3	46.948	618.005

Table 6.2 – RSS for the final model.

We see that including the phase 3 of the load signal improves both the baseline and the final model. Though, compared to Transformer 1 we still have a considerable higher RSS.

Appendix B

In this appendix we extend the analysis of our prediction errors by including 24- and 48-step ahead RSS values. For the four main models (each found in a section called final model) we obtain:

		RSS			
Transformer	States	1-step ahead	12-step ahead	24-step ahead	48-step ahead
1	1	16.16	416.86	640.04	662.31
1	2	16.08	413.30	636.18	661.55
2	1	52.81	775.49	990.20	1004.91
2	2	51.72	653.37	812.73	827.73

Table 6.3 – n-step ahead predictions for our four final models, where we let $n \in \{1, 12, 24, 48\}$. All results are found without relaxing the system variance.

As expected the prediction error increases, when n increases. We see that the performance of each model relatively varies for the different steps. Finally, we see in table 6.3 that adding a second state only drastically improve our model with respect to Transformer 2.

Appendix C

In appendix C we include all parameters needed for producing our optimal fits. The models for which the parameters are shown are similar to the ones include in Appendix B.

Final Model - Transformer 1 one state

Parameters	Estimate	t value	P-value
Ti0	2.85e+01	649.57	<2.2e-16
a	7.99e+01	214.94	<2.2e-16
b	1.94e+01	38.02	<2.2e-16
c	3.94e+01	806.30	<2.2e-16
Ce	1.66e+03	39.68	<2.2e-16
Ct	7.82e+04	3591.85	<2.2e-16
e11	-4.57e+01	-56905.38	<2.2e-16
p11	-6.80e+00	-33504.26	<2.2e-16
Ria	3.31e+01	38.30	<2.2e-16
sc1	2.39e+00	21.52	<2.2e-16
sc2	-1.22e+00	-17.11	<2.2e-16
sc3	3.04e+00	21.77	<2.2e-16
sc4	-3.81e+00	-19.75	<2.2e-16
w1	-4.22e-01	-26.62	<2.2e-16
w2	-1.98e-01	-26.89	<2.2e-16
w3	-2.57e-01	-29.98	<2.2e-16
w4	-3.49e-01	-32.10	<2.2e-16

Note here that e11 and p11 (respectively ε and σ in our report) are log transformed in our optimization. Both Ce and Ct are included instead of C_ℓ to smooth the optimization.

Final Model - Transformer 1 two state

Parameters	Estimate	t value	P-value
Ti0	2.85e+01	7.74e+02	<2.2e-16
Tt0	4.63e+01	1.12e+04	<2.2e-16
a	3.82e+00	1.77e+02	<2.2e-16
b	9.57e-01	4.91e+01	<2.2e-16
c	3.83e-02	5.18e+03	<2.2e-16
Ce	3.76e+03	1.80e+02	<2.2e-16
e11	-4.56e+01	-1.16e+05	<2.2e-16
p11	-7.17e+00	-8.48e+04	<2.2e-16
p22	-7.18e+00	-3.37e+06	<2.2e-16
Ria	1.43e+01	9.46e+01	<2.2e-16
Rti	1.81e+01	4.38e+03	<2.2e-16
sc1	5.59e+00	2.38e+01	<2.2e-16
sc2	-2.89e+00	-1.72e+01	<2.2e-16
sc3	7.06e+00	2.39e+01	<2.2e-16
sc4	-8.83e+00	-2.00e+01	<2.2e-16
w1	-9.87e-01	-2.83e+01	<2.2e-16
w2	-4.48e-01	-2.84e+01	<2.2e-16
w3	-5.95e-01	-3.98e+01	<2.2e-16
w4	-8.07e-01	-4.63e+01	<2.2e-16

Here p11 and p22 denote respectively σ_1 and σ_2.

Final Model - Transformer 2 one state

Coefficients	Estimate	t value	P-value
Ti0	2.82e+01	595.69	<2.2e-16
a	2.37e+02	206.66	<2.2e-16
b	6.64e+01	69.56	<2.2e-16
c	1.04e-09	98.94	<2.2e-16
Ce	1.17e+03	83.96	<2.2e-16
Ct	9.76e+04	1123.87	<2.2e-16
e11	-4.58e+01	-20550.29	<2.2e-16
p11	-6.80e+00	-64821.47	<2.2e-16
Ria	2.09e+01	78.21	<2.2e-16
sc1	3.11e+00	17.54	<2.2e-16
sc2	-1.95e+00	-15.33	<2.2e-16
sc3	4.55e+00	18.56	<2.2e-16
sc4	-6.39e+00	-16.535	<2.2e-16
w1	-6.46e-01	-31.09	<2.2e-16
w2	-2.31e-01	-26.44	<2.2e-16
w3	-3.72e-01	-31.33	<2.2e-16
w4	-3.77e-01	-36.79	<2.2e-16

Final Model - Transformer 2 two state

Parameters	Estimate	t value	P-value
Ti0	2.82e+01	7.39e+02	<2.2e-16
Tt0	4.67e+01	3.60e+03	<2.2e-16
a	3.30e+00	1.09e+02	<2.2e-16
b	7.72e-01	6.81e+01	<2.2e-16
c	1.11e-01	3.75e+01	<2.2e-16
Ce	1.52e+03	1.16e+02	<2.2e-16
e11	-4.57e+01	-9.68e+04	<2.2e-16
p11	-6.80e+00	-4.03e+05	<2.2e-16
p22	-7.18e+00	-2.78e+06	<2.2e-16
Ria	1.46e+01	1.06e+02	<2.2e-16
Rti	5.73e+01	3.45e+01	<2.2e-16
sc1	3.20e+00	1.26e+01	<2.2e-16
sc2	-2.29e+00	-1.32e+01	<2.2e-16
sc3	5.86e+00	1.81e+01	<2.2e-16
sc4	-8.84e+00	-1.77e+01	<2.2e-16
w1	-8.97e-01	-3.07e+01	<2.2e-16
w2	-3.45e-01	-2.98e+01	<2.2e-16
w3	-5.11e-01	-3.42e+01	<2.2e-16
w4	-5.33e-01	-3.95e+01	<2.2e-16

Bibliography

[1] "ctsmr - continuous time stochastic modelling for r." [Online]. Available: http://ctsm.info/

[2] "Three-phase electric power." [Online]. Available: https://en.wikipedia.org/wiki/Three-phase_electric_power

[3] "Elforsyning." [Online]. Available: https://denstoredanske.lex.dk/elforsyning

[4] H. Madsen, *Time series analysis*. Chapman and Hall/CRC, 2007.